



HAL
open science

Land water storage variability over West Africa estimated by GRACE and land surface models

Manuela Grippa, Laurent Kergoat, Frédéric Frappart, Quentin Araud, Aaron Boone, Patricia de Rosnay, Jean-Michel Lemoine, Simon Gascoin, G. Balsamo, Catherine Otle, et al.

► **To cite this version:**

Manuela Grippa, Laurent Kergoat, Frédéric Frappart, Quentin Araud, Aaron Boone, et al.. Land water storage variability over West Africa estimated by GRACE and land surface models. *Water Resources Research*, 2011, 47 (5), pp.W05549. <10.1029/2009WR008856>. <hal-00649833>

HAL Id: hal-00649833

<https://hal.science/hal-00649833v1>

Submitted on 8 Dec 2011

HAL is a multi-disciplinary open access archive for the deposit and dissemination of scientific research documents, whether they are published or not. The documents may come from teaching and research institutions in France or abroad, or from public or private research centers.

L'archive ouverte pluridisciplinaire **HAL**, est destinée au dépôt et à la diffusion de documents scientifiques de niveau recherche, publiés ou non, émanant des établissements d'enseignement et de recherche français ou étrangers, des laboratoires publics ou privés.



HAL Authorization

1 Land water storage variability over West Africa
2 estimated by GRACE and land surface models

M. Grippa,¹ L. Kergoat,¹ F. Frappart,¹ Q. Araud,¹ A. Boone,² P. de Rosnay,³

J.-M. Lemoine,⁴ S. Gascoin,⁵ G. Balsamo,³ C. Ottlé,⁶ B. Decharme,² S.

Saux-Picart⁷ and G. Ramillien¹

Q. Araud, Géosciences Environnement Toulouse (UMR 5563, CNRS- Université Toulouse III-IRD), 14 av. E. Belin, 31400, Toulouse, France. (araud.quentin@gmail.com)

G. Balsamo, European Centre for Medium-Range Weather Forecasts, Shinfield Park, Reading, RG2 9AX, U.K. (Gianpaolo.Balsamo@ecmwf.int)

A. Boone, Centre National de Recherches Météorologiques, 42, av. G. Coriolis, 31057, Toulouse, France. (aaron.boone@meteo.fr)

B. Decharme, Centre National de Recherches Météorologiques, 42, av. G. Coriolis, 31057, Toulouse, France. (bertrand.decharme@cnrm.meteo.fr)

F. Frappart, Géosciences Environnement Toulouse (UMR 5563, CNRS- Université Toulouse III-IRD), 14 av. E. Belin, 31400, Toulouse, France. (frappart@get.obs-mip.fr)

S. Gascoin, Centro de Estudios Avanzados en Zonas Aridas, Calle Benavente 980, La Serena, Chile. (simon.gascoin@ceaza.cl)

M. Grippa, Géosciences Environnement Toulouse (UMR 5563, CNRS- Université Toulouse III-IRD), 14 av. E. Belin, 31400, Toulouse, France. (manuela.grippa@get.obs-mip.fr)

L. Kergoat, Géosciences Environnement Toulouse (UMR 5563, CNRS- Université Toulouse III-IRD), 14 av. E. Belin, 31400, Toulouse, France. (laurent.kergoat@get.obs-mip.fr)

J-M. Lemoine, Dynamique Terrestre et Planétaire (UMR 5562, CNRS- UPS Toulouse III), 14 av. E. Belin 31400, Toulouse, France. (jean-michel.lemoine@cnes.fr)

C. Ottlé, Laboratoire des Sciences du Climat et de l'Environnement LSCE/IPSL/CEA-CNRS-UVSQ Centre d'Etudes de Saclay, Orme des Merisiers 91191 Gif-sur-Yvette, France. (cather-

3 **Abstract.**

4 Land water storage plays a fundamental role on the West African water
5 cycle and has an important impact on climate and on the natural resources
6 of this region. However, measurements of land water storage are scarce at
7 regional and global scales and, especially, in poorly instrumented endhoreic
8 regions, such as most of the Sahel, where little useful information can be de-
9 rived from river flow measurements and basin water budgets.

10 The GRACE satellite mission provides an accurate measurement of the
11 terrestrial gravity field variations from which land water storage variations
12 can be derived. However, their retrieval is not straightforward, and differ-
13 ent methods are employed which result in different water storage GRACE
14 products. On the other hand, water storage can be estimated by land sur-
15 face modelling forced with observed or satellite-based boundary conditions,
16 however such estimates can be highly model dependent.

ine.ottle@lsce.ipsl.fr)

G. Ramillien, Géosciences Environnement Toulouse (UMR 5563, CNRS- Université Toulouse
III- IRD), 14 av. E. Belin, 31400, Toulouse, France. (Guillaume.Ramillien@get.obs-mip.fr)

P. de Rosnay, European Centre for Medium-Range Weather Forecasts, Shinfield Park, Reading,
RG2 9AX, U.K. (patricia.Rosnay@ecmwf.int)

S. Saux-Picart, Plymouth Marine Laboratory, Prospect Place, The Hoe, Plymouth PL1 3DH,
U.K. (stux@pml.ac.uk)

17 In this study, land water storage by six GRACE products and soil mois-
18 ture estimations by nine land surface models (run within the framework of
19 the AMMA Land Surface Intercomparison Project, ALMIP) are evaluated
20 over West Africa, with a particular focus on the Sahelian area. The water
21 storage spatial distribution, including zonal transects, its seasonal cycle and
22 its inter annual variability are analysed between 2003 and 2007. Despite the
23 non-negligible differences among the various GRACE products and among
24 the different models, a generally good agreement between satellite and model
25 estimates is found over the West Africa study region. In particular, GRACE
26 data are shown to reproduce well the water storage inter annual variability
27 over the Sahel for the 5-year study period. The comparison between satel-
28 lite estimates and ALMIP results lead to the identification of processes need-
29 ing improvement in the land surface models. In particular, our results point
30 out the importance of correctly simulating slow water reservoirs as well as
31 evapotranspiration during the dry season for accurate soil moisture modelling
32 over West Africa.

1. Introduction

33 Land water storage plays a fundamental role within the global water cycle and on cli-
34 mate, particularly in regions where the coupling between land surface and the atmosphere
35 is theorized to be important such as West Africa [*Koster et al.* , 2004]. In this region, land
36 processes related to soil moisture and vegetation have been shown to have an important
37 impact on the development of the summer monsoon, by amplifying its response to oceanic
38 forcing [*Giannini et al.* , 2003, 2008]. Monitoring water storage changes over this region
39 is therefore fundamental for better understanding land-atmosphere processes as well as
40 evapotranspiration related processes. In addition, given the possible link between soil
41 moisture and the atmosphere, improved knowledge of water storage which is a relatively
42 slow varying component in the climate system, could lead to improved long term pre-
43 dictions [*Philippon and Fontaine* , 2002]. Moreover, in West Africa, and particularly in
44 the Sahel, water storage changes directly affect the natural resource availability, therefore
45 they have a significant environmental and socio-economic impact. Water storage is a key
46 variable for evaluating the past and present state of natural resources such as water and
47 fodder and to model their future development within the context of climate change.

48 However, direct measurements of land water storage are not readily available at regional
49 and global scales. This is true especially in the Sahel, where monitoring the water budget
50 components is not easy due to the scarcity of in situ measurements especially in terms
51 of precipitation. Even when local measurements are available, it remains difficult to
52 extrapolate them over larger areas given the relatively large spatial heterogeneity of the
53 main components of the terrestrial water cycle (see for example *Lebel et al.* [1997].)

54 Moreover, little useful information on water storage can be derived from river discharge
55 measurements since this region is mostly endhoreic, i.e., the main West African water
56 basins are not fed by Sahelian waters.

57 The GRACE satellite mission provides an accurate measurement of terrestrial gravity
58 field variations from which land water storage variations can be derived. As opposed to
59 microwave passive and active spaceborne sensors that can be used to retrieve surface soil
60 moisture in the uppermost few centimetres, GRACE data can be used to estimate water
61 storage variations integrated over the entire water column, including the root zone as well
62 as deeper groundwater reservoirs. The retrieval of the terrestrial water storage (TWS)
63 from the satellite gravity measurements is not straightforward and requires solving an
64 ill-posed inverse problem. Different methods are employed to do this by various research
65 teams [*Chambers* , 2006; *Rowlands et al.* , 2005; *Liu* , 2008; *Bruisma et al.* , 2010;
66 *Ramillien et al.* , 2005] that provide different GRACE water storage estimates [see for
67 example, *Klees et al.* , 2008a] .

68 Since the satellite launch in 2002, GRACE data have been increasingly used for different
69 hydrological applications [among others, *Ramillien et al.* , 2008a; *Schmidt et al.* , 2008],
70 for example the monitoring of extreme hydrological events [*Chen et al.* , 2009; *Seitz et al.* ,
71 2008; *Andersen et al.* , 2005], for evaluating hydrological fluxes such as evapotranspiration
72 [*Rodell et al.* , 2004; *Ramillien et al.* , 2006], to compute atmospheric water vapour
73 convergence [*Swenson and Wahr* , 2006] and reiver discharge [*Syed et al.* , 2005], as well
74 as for integrated water budget studies [*Yirdaw et al.* , 2008; *Crowley et al.* , 2006].

75 Evaluation of the seasonal and interannual variability of the GRACE water storage
76 estimates has been mainly carried out over well defined water basins at regional or global

77 scales. GRACE water storage products have been compared to in-situ measurements
78 using soil moisture networks [*Swenson et al* , 2008], to well level data combined with
79 hydrological models [*Schmidt et al.* , 2008] and to modelling results [e.g., *Schmidt et al.*
80 , 2006; *Papa et al.* , 2008; *Syed et al.* , 2008; *Schmidt et al.* , 2008; *Klees et al.* , 2008a].
81 GRACE data have also been used to provide useful information for calibrating and/or
82 improving the water storage simulation in land surface models [*Ngo-Duc et al.* , 2007;
83 *Niu et al.* , 2007; *Güntner et al.* , 2008; *Syed et al.* , 2008; *Alkama et al.* , 2009].

84 Until recently, only a few GRACE studies have been carried out over west Africa, despite
85 the fact that several global studies included the Niger river basin [e.g., *Papa et al.* , 2008;
86 *Schmidt et al.* , 2008; *Ramillien et al.* , 2008b; *Syed et al.* , 2008; *Ngo-Duc et al.* , 2007].
87 No extensive evaluation of GRACE water products has been performed for the Sahel, and
88 more generally, for endhoreic areas. Moreover, the capability of GRACE to reproduce the
89 interannual variability of water storage changes over West Africa has not been specifically
90 addressed.

91 The objective of this work is to better understand the intra seasonal and interannual
92 variability of the water cycle over West Africa, and in particular, the Sahel. This is
93 done by using GRACE TWS products as well as soil moisture derived by an ensemble of
94 land surface models participating in the AMMA Land Surface Intercomparison Project
95 [ALMIP, *Boone et al.* , 2009]. For the time period 2003-2007, satellite products and models
96 outputs are analysed and compared considering different aspects of the continental water
97 storage: the seasonal cycle (amplitude and phase), the interannual variability during the
98 wet and dry season and the zonal distribution.

1.1. Study area

99 The study area is the West African region bordering the Guinean gulf to the South and
100 the Sahara desert to the North (Fig. 1). The analysis is carried out over two arbitrary
101 areas: the "West Africa" box between 10°W - 10°E and 6°N - 18°N and the "Sahel" box
102 between 10°W - 10°E and 12°N - 18°N .

103 West Africa is characterized to a good approximation by a zonal distribution of pre-
104 cipitation and land cover. The annual precipitation gradient ranges from about 1000
105 mm/year in the Guinean zone to 100 mm/year to the north of the Sahelian region. The
106 precipitation annual cycle (Fig. 2) is driven by the West African monsoon, and it is
107 related to the meridional displacement of the Inter tropical Convergence Zone [ITCZ,
108 *Sultan and Janicot* , 2003]. It reaches 5°N in April and stays in a quasi-stable position
109 until the end of June, then it abruptly shifts during the first half of July to 10°N , where
110 it remains until the end of August. Over the Sahel, the rainy season peaks between July
111 and September. The ITCZ gradually withdraws southward from September to November
112 which is associated with a sharp precipitation decrease over this region.

113 The West African hydrological systems are also roughly organised as a function of the
114 latitudinal gradient, with significant water lateral transfers within deeper soil layers in
115 the southern areas, and hortonian systems, characterised by superficial water flow, to the
116 north [*Peugeot et al.* , 1997; *Braud et al.* , 1997]. Southern areas are mostly exohreic
117 with considerable sheet run-off. The hydrological system become progressively endhoreic
118 going northward, where, depending on the soil properties, endhoreic sandy soils alternate
119 with smaller areas characterised by concentrated run-off. The Sahel is dominated by large
120 old sedimentary basins consisting in either deep fossil aquifers or less deep, more or less

121 fragmented, actively recharged aquifers which are affected by minor seasonal fluctuations
122 and decadal trends [Favreau *et al.*, 2009]. The southern half of the West African box is
123 dominated by the African Shield with shallow fragmented aquifers which have variations
124 that follow the seasonal pattern of rainfall and river drainage.

125 The vegetation gradient follows the precipitation pattern: going from south to north,
126 the dominant vegetation consists of forest, savannah and parkland, grassland and open
127 shrub lands. Crops and fallows are also present and they are scattered throughout the
128 study region.

129 The largest river in the Sahel is the Niger, but the majority of the Sahel box is endhoreic
130 and does not feed the Niger River [Descroix *et al.* , 2009]. The run-off seasonal evolution
131 is delayed compared to the precipitation seasonal cycle. The maximum run-off enters and
132 exits the Sahel box in September and the river flow decreases after the rain season at a
133 slower rate than precipitation. The Inner Niger delta, an area of swamps and small lakes
134 in the Sahelian region in Mali, typically floods during the wet season and is subject to
135 intense evaporation, further delaying the Niger discharge seasonal cycle.

2. Data and methods

2.1. GRACE data

136 The Gravity Recovery and Climate Experiment (GRACE) satellite mission, managed by
137 NASA and DLR, has been collecting data since mid-2002. Estimates of the Earth's gravity
138 field produced by GRACE can be used to infer changes in mass at and below the surface of
139 the Earth, including the oceans, the polar ice sheets, the land water storage (surface water,
140 soil moisture, snow and ground water) and the solid Earth. To extract land water storage
141 changes on a given region of the Earth, two issues need to be addressed: 1- the contribution

142 of atmospheric, oceanic, and solid earth mass variations need to be separated from the
143 hydrological signal, which generally requires the employment of background models ; 2-
144 the TWS signal over a given region of the earth needs to be separated from contaminations
145 coming from a different region, such as the water storage variability in a neighbouring area
146 or ocean.

147 In this study, six different GRACE products (table 1) are employed and briefly described
148 below.

- 149 • The three monthly land water solutions (RL04) provided by the GeoForschungsZen-
150 trum, Potsdam (GFZ), the Jet Propulsion Laboratory, California Institute of Technology
151 (JPL), and the Center for Space Research , University of Texas at Austin (CSR), with a
152 spatial resolution of 400 km, available at <ftp://podaac.jpl.nasa.gov/tellus/grace/monthly>.
153 These three datasets are processed as reported by *Chambers* [2006]. Each monthly grav-
154 ity field is represented by a set of spherical harmonic (Stokes) coefficients, developed to
155 degree and order 60. CSR, GFZ, and JPL use different algorithms to compute gravity
156 field harmonic coefficients from the raw GRACE observations, although they have agreed
157 to use similar background models for the ocean and the atmosphere. Spatial averaging,
158 or smoothing, of GRACE data is commonly used to reduce the anisotropic noise, which
159 manifests itself in strong north-south stripes. Systematic errors causing the longitudinal
160 stripes, identified by correlations between spherical harmonic coefficients of like parity
161 within a particular spectral order, are removed using the destriping method described by
162 *Swenson and Wahr* [2006b]. After destriping, the signal can be further smoothed using a
163 Gaussian filter of a certain radius. For the comparison to the ALMIP results, in this study
164 we employ the destriped but unfiltered solutions. However, solutions smoothed with a

165 Gaussian filter of radius equal to 500 and 300 km are also analysed in section 2.1.1 in
166 order to better investigate the effects of filtering.

167 • The DEOS Mass Transport Model (DMT-1) monthly solutions by the University of
168 Delft available at <http://www.lr.tudelft.nl>. The DMT-1 is also based on the decomposition
169 into spherical harmonic Stokes coefficients to degree and order 120. The details of the
170 computation of monthly solutions and corresponding covariance matrices are given by
171 *Liu* [2008]. The series of monthly solutions is post-processed by applying statistically
172 optimal Wiener filters based on full signal and noise covariance matrices instead of a
173 Gaussian filter. The signal variances and solutions are computed iteratively, according to
174 the scheme described by *Klees et al.* [2008b].

175 • The Level-2 GRGS-EIGEN-GL04 10 day models derived from GRACE GPS
176 and K-band range-rate data and from LAGEOS-1/2 SLR data [*Bruisma et al.* ,
177 2010] available at <http://grgs.obs-mip.fr/index.php/fre/Donnees-scientifiques/Champ-de-gravite/grace/release02>. These gravity fields are expressed in terms of normalized spher-
178 ical harmonic coefficients from degree 2 up to degree 50 using a stabilization approach
179 without additional filtering. We use the TWS 10-day grids with a spatial resolution of 1°
180 $\times 1^\circ$ from January 2003 to December 2007.

182 • The 10 day land water solutions from GSFC, with a spatial resolution of $4^\circ \times 4^\circ$,
183 available for the period April 2003- April 2007 at <http://grace.sgt-inc.com/>. The data are
184 processed with an approach based on a local time-dependent mass recovery using mass
185 concentrations blocks [*Mascons, Rowlands et al.* , 2005] rather than using global basis
186 functions such as spherical harmonics. The formulation for Mascons solutions exploits
187 the fact that a change in potential caused by adding a small uniform layer of mass over a

188 region at a time t , can be represented as a set of (differential) potential coefficients which
189 can be added to the mean background field. Mascons can be located in space, and hence,
190 short wavelength errors (e.g. due to ocean tides) should not leak into land areas, although
191 spatial constraints are imposed on neighbouring $4^\circ \times 4^\circ$ pixels.

192 In the following study, the water storage anomalies (reported in mm) have been re-
193 centered for each solution by removing the mean over the 2003-2006 common period.

194 **2.1.1. Filtering and leakage**

195 Several recent studies have shown that GRACE data over the continents provide infor-
196 mation on the total land water storage with an accuracy between 15 and 30 mm of liquid
197 water thickness equivalent [*Schmidt et al.* , 2006; *Llubes et al.* , 2007; *Klosko et al.* ,
198 2009], depending on the region considered.

199 GRACE water storage estimates at a given location are affected by data processing
200 which requires a compromise between maximising spatial resolution and reducing noise.
201 This is done following different approaches, such as, for example:

- 202 • truncating the harmonical series computation at a given degree (50, 60 or 120, the
203 lower the degree, the greater the smoothing) as done for all the products considered here
204 except the Mascons (CSR, JPL and GFZ truncating at degree 60, CNES at 2 to 50 and
205 DMT at 120) ;
- 206 • applying smoothing filters, such as the Gaussian filtering with the radius of 300 and
207 500 km used by the CSR, JPL and GFZ post-processed solutions or the optimal Wiener
208 filter used in the DMT-1 model;
- 209 • employing stabilisation approaches such as that used for the CNES solution;
- 210 • imposing spatial constraints as done for the Mascon solutions.

211 All of these approaches make the water storage estimates in a given region biased and
212 sensitive to mass changes outside the region of interest (leakage). Leakage is comprised of
213 to mechanisms: a) leakage of signal from the target area to the surroundings (leakage out),
214 and b) leakage of signal from the surroundings into the target area (leakage in). In this
215 paper, we employ the term leakage to mean both mechanisms (leakage in and out), even
216 if sometimes this term is used to described the mechanism b) only. A survey of different
217 methods employed to take into account leakage effects can be found in *Longuevergne et*
218 *al.* [2010]. *Chen et al.* [2005] showed that if temporal water storage variations are
219 homogeneous over a sufficiently large area, leakage in and out may partially cancel each
220 other, minimising the overall leakage effect. On the contrary, leakage effects are expected
221 to have the highest impact when mass changes inside the study region are in opposition of
222 phase with mass changes outside it. For basins surrounded by areas with smaller storage
223 variations (oceans, deserts) the effects of leakage should therefore make the effective water
224 storage underestimated.

225 Fig. 3 shows, for each product, the spatial distribution of water storage anomalies in
226 September, the month of the maximum soil water over West Africa. To illustrate the
227 impact of using a Gaussian filter in the post-processing, CSR, JPL and GFZ solutions
228 smoothed by a Gaussian filter of 500 km radius are also shown. All GRACE estimates
229 indicate a maximum, more or less pronounced, at the south-east corner of the study
230 area and another maximum at a latitude of about 12° N but at different longitudes for
231 different products. In addition, CSR, JPL and GFZ at 500 km appears much smoother
232 than the same unfiltered solutions. However the latter solutions show the effects of residual
233 longitudinal stripes not completely eliminated by the destriping process by *Swenson and*

234 *Wahr* [2006b]. Alternative destriping methods [*Frappart et al.*, 2011; *Klees et al.*, 2008b;
235 *Kusche*, 2007], which are more efficient for equatorial areas, may be applied. However,
236 in this study, these effects are not a major problem given that we analyse water storage
237 changes averaged over a sufficiently large longitudinal domain.

238 Regarding the seasonal dynamics, Fig. 4 shows the comparison between the CSR, JPL
239 and GFZ solutions (multi-product mean) post-processed by a Gaussian filter with a 500
240 km radius and the corresponding solutions without any Gaussian filtering. Over the
241 West African box, filtered data show a lower dynamic than the unfiltered data, which is
242 consistent with the geographic configuration, West Africa being surrounded by areas with
243 small seasonal dynamics (ocean, Sahara desert). Conversely, for the Sahel box, the 500 km
244 Gaussian filter slightly increases the seasonal dynamics. This implies that contamination
245 from the Soudanian area, located to the South of the Sahel box, more than compensates
246 damping effect from the Sahara desert at the Northern border. Differences between the
247 monthly TWS values of smoothed and unsmoothed solutions are no more than 10-15 mm
248 for both regions but are more significant at about 10° where CSR, JPL and GFZ unfiltered
249 solutions are more coherent with the other solutions analysed (CNES, DMT et GSFC)
250 than the CSR, JPL and GFZ solutions post-processed using a Gaussian filter (not shown).

251 Leakage resulting from the combined effects of Gaussian filtering, destrip-
252 ing and truncating the harmonical series, can be estimated from hydrologi-
253 cal models, as done for example by *Klees et al.* [2007] and by Swenson
254 (ftp://podaac.jpl.nasa.gov/pub/tellus/grace_monthly/swenson_destripe/ss201008/) who
255 propose correcting factors to account for this. This is estimated here for the CSR, JPL and
256 GFZ solutions following the method by Swenson that calculates a correcting factor on a

257 one degree grid basis by using a global simulation of land hydrology. The simulated TWS
258 field underwent the same processing as the RL04 data: spherical harmonical expansion,
259 truncation to degree 60 and destriping. The data were then post processed using a 300
260 km Gaussian filter, and then regressed against the original TWS. The regression slope can
261 then be used as a correction factor for the GRACE data. This correction, accounting for
262 leakage out and leakage in, is shown in Fig. 5 for the West Africa and the Sahel boxes. It
263 has very similar effects to those attributed to the application of the Gaussian filter alone
264 (Fig. 4), with the GRACE seasonal dynamics enhanced over West Africa and reduced
265 for the Sahel box. A similar calculation with another hydrological model following the
266 method by *Ramillien et al.* [2008b] (not shown) resulted in a slightly higher leakage over
267 the Sahel box.

268 In conclusion, the above estimates of leakage errors imply that, for global solutions,
269 water storage changes are probably underestimated for the West Africa box, whereas they
270 may be slightly overestimated for the Sahel box. A complete error budget should also
271 address the data and inversion errors, which are not known precisely. In this analysis,
272 we do not apply explicit corrections to account for leakage effects given that they are
273 dependent on hydrological models and on the methodology followed to calculate them.
274 Our approach is therefore to inter-compare the different GRACE solutions to have a rough
275 idea of GRACE processing errors.

276 The temporal evolution of the TWS by all the GRACE products considered, spatially
277 averaged over the West African and the Sahelian boxes (given its coarser resolution the
278 GSFC product has been averaged over slightly larger boxes, with latitudes between 4°N
279 - 20°N for West Africa, and 12°N - 20°N for the Sahel, and longitudes between 12°W -

280 12°E) is shown in Fig. 6. The six products are quite consistent regarding their temporal
281 evolutions, with water storage maxima generally found in September and minima in April
282 (West Africa) and May (Sahel). A temporal shift is sometimes observed with respect to
283 the date at which the maxima and minima are reached : this is not systematic for a given
284 product and it is more important for the dates of the water storage minima for which
285 the shift can be up to 2 months (as for example over the Sahel in 2007). In term of the
286 amplitudes of the seasonal water storage changes (for each year, the difference between the
287 maximum and minimum value), the 6 GRACE products show significant differences, with
288 the CNES and CSR solutions generally higher and GFZ lower than the other solutions.
289 Year to year variations are also observed among the different solutions.

2.2. ALMIP models

290 The ALMIP model inter comparison [*Boone et al.* , 2009] was carried out by run-
291 ning different state-of-the-art land surface models using the same forcing database, which
292 consists in atmospheric state variables, precipitation and incoming radiative fluxes. The
293 atmospheric state variables were derived form ECMWF short term forecast data, while
294 downwell radiative fluxes were a mix of ECMWF and LANDSAF estimates.

295 For the simulation of the different components of the water budget, the most crucial
296 forcing variable is precipitation. In this study, we used the simulations forced by the Trop-
297 ical Rainfall Measurement Mission (TRMM) precipitation product 3B-42 [*Huffman et al.* ,
298 2007] (see Fig. 2). Nine different models which are made for climate or numerical weather
299 prediction (such as for example SSIB, NOHA, HTESEL, ISBA and ORCHIDEE), or
300 more hydrologically based models (such as for example CLSM) participated in this inter
301 comparison (table 2). These models have different degrees of complexity in terms of the

302 representation of the water budget variables, such as, for example, the number of verti-
303 cal soil layers and the soil depth over which vertical water transfers are simulated (for
304 more details see *Boone et al.* [2009]). Among the ALMIP models, CLSM is the only
305 model including a representation of a saturated area following the TOPMODEL concept.
306 Land surface parameters concerning soil and vegetation are taken from the ECOCLIMAP
307 database for all models except for HTESSEL and SSIB.

308 The time change in soil moisture, ΔS , vertically integrated over all of the soil layers,
309 is the output variable considered in the following analysis for comparison with GRACE
310 water storage change. It is related to the other water budget variables (input precipitation,
311 P , evapotranspiration, E and total run-off, including surface run-off and drainage, R , in
312 mm/hour) by the following equation:

$$\frac{dS}{dt} = P - E - R$$

313 ΔS is calculated in the ALMIP experiment over a time interval of 3 hours. Mean an-
314 nual values for the variables on the right hand side of the above equation are reported in
315 Table 3. Simulated evapotranspiration is very significant over the Sahel, accounting for
316 85% of input precipitation on average (multi models average for the whole study period).
317 Total run-off is much less, with surface run-off accounting for 6 % and drainage for 8.5%
318 of input precipitation. Total run-off is more significant in the Southern part of the study
319 area, where it is 30% of input precipitation, while evapotranspiration accounts for 70 %
320 of input precipitation between 6° N and 12° N. However, the partitioning between evap-
321 otranspiration and total run-off is quite variable among different models: over the West
322 Africa region, average yearly simulated evapotranspiration ranges from a minimum value
323 of 482 mm/year for the SSIB1 model to a maximum of 677 mm/year for the HTESSEL

324 model. Total run-off ranges from a minimum value of 95 mm/year for the HTESSEL
325 model to a maximum of 317 mm/year for the SSIB1 model.

326 As done for the GRACE products, ΔS has been integrated over time to obtain monthly
327 soil moisture and then transferred to anomalies by removing the mean over the 2003-2006
328 period.

329 The spatial distribution of soil moisture anomalies for the different ALMIP models in
330 September is shown in Fig. 7. All models have a soil moisture maximum to the south-east
331 corner of the study area and this is more evident for HTESSEL, ORCHIDEE and JULES
332 than for the other models. Another area of high soil moisture, more or less pronounced,
333 is found by the majority of models at about 12°N and 5°W. Fig. 8 shows the temporal
334 variability of modelled water storage spatially averaged over the West Africa and the
335 Sahel boxes for the nine land surface models considered. The temporal changes are very
336 coherent among the different models and the dry and wet phases are well represented.
337 This is perhaps not surprising since soil moisture changes are primarily determined by
338 the precipitation events that are the same for all models. However, large differences
339 among the model simulations can be observed during the drying phase following the rainy
340 season. Differences in the parametrisations employed by different land surface models are
341 indeed enhanced in this period compared to the wetting phase when the water storage
342 simulation is more constrained by the input precipitation. Significant differences of soil
343 moisture seasonal amplitudes among different models are also observed.

3. Results

344 In the following section, the spatial and temporal distribution of water storage anomalies
345 by GRACE and soil moisture anomalies by ALMIP are analysed.

346 Given the scatter among different GRACE water storage estimations as well as among
347 different model results, the comparison between GRACE products and ALMIP results
348 does not allow the determination of 'the best' GRACE products or 'the best' land sur-
349 face model. Therefore, in the following analysis, results are first presented as mean and
350 standard deviation values for the 6 GRACE products compared to mean and standard
351 deviation values for the 9 ALMIP models considered.

352 Fig. 9 shows the temporal evolution of the mean GRACE and the mean ALMIP water
353 storage anomalies over the 2003-2007 period. A general agreement is found between satel-
354 lite and model estimations: the wet and dry phases are distinguished well in both cases,
355 and water storage mean amplitudes are quite similar. The overall agreement between
356 GRACE and models is worse during the dry season: GRACE products show a strong
357 interannual variability that is not observed for the ALMIP models in the dry season.
358 Moreover, a water storage increase during the dry season (January to March) is some-
359 times observed in the GRACE data, particularly in 2005, but also in 2007 and to a lesser
360 extent in 2006. This increase, detected by all of the GRACE products (fig. 4), is unlikely
361 related to the data processing methodology, but its causes remain unclear.

362 The comparison between satellite and model outputs has to be carried out carefully since
363 the two estimates are not completely equivalent. Water storage estimates by GRACE do
364 take into account soil water integrated over the entire soil depth, therefore including
365 aquifers as well as surface water contained within river beds and floodplains. In the land
366 surface models employed here, the entire "hydrologically active" soil depth is represented
367 by a shallow soil reservoir. In addition there is no water transfer between adjacent cells
368 and drainage through the deepest soil limit is lost. No explicit treatment of river water

369 and floodplains is taken into account in this study. The comparison is therefore valid if
370 these effects are not significant over the study area.

371 As detailed in the following subsection, for the Sahel box, we have calculated the con-
372 tribution of water in the Niger River (the largest river of the Sahel box) and in the Niger
373 delta to the seasonal variations of equivalent water height.

374 The effects of aquifers and the water table are much more difficult to quantify given the
375 scarcity of information of these variables at a regional scale and the large heterogeneity
376 of underground systems in West Africa. In this sense, GRACE may provide missing
377 information that is otherwise difficult to quantify. If all the other sources of discrepancies
378 are accounted for, one can argue that the differences between GRACE and ALMIP gives
379 an indication of water table variability.

3.1. Niger River and Niger delta contribution

380 The Niger River loses water through evaporation when flowing in the Sahelian zone
381 because of the large floodplain known as the Mali wetland or the Niger inner delta and
382 also because a large part of the basin consists of endhoreic systems, which do not con-
383 tribute water to the river [*Descroix et al.*, 2009]. Water mass variations have been
384 estimated using satellite altimetry data for the Niger River and from literature for the
385 Niger delta. As detailed in the appendix, records of 12 altimetry-derived water levels from
386 the Hydroweb website (<http://www.legos.obs-mip.fr/en/soa/hydrologie/hydroweb>) based
387 on measurements from Topex/Poseidon, Jason-1, ERS-2, ENVISAT and GFO, have been
388 combined to estimates of the river width to derive variations in the river water mass. For
389 the inner delta, the mass of water has been estimated by the difference in river discharge
390 at Dire (outlet) and Douna and Kirango (upstream) from the Global Runoff Data Center

391 (<http://www.grdc.sr.unh.edu/>), subtracting evaporation losses within the delta (see the
392 appendix).

393 Fig. 10 shows the Niger River and Niger delta TWS (mm) anomaly for the Sahel box.
394 The main contribution is due to the delta, with a seasonal amplitude of -4 to 6 mm while
395 the river water mass varies between -2 and 2 mm. Due to the delay caused by the slow
396 water progression in the floodplain, the Niger flood peak shifts from August to December
397 when flowing in the Sahel box, which attenuates the seasonal cycle of the total mass
398 variation. The contribution of the other rivers in the Sahel box is expected to be, at
399 most, of the same magnitude as the Niger river, with a seasonal cycle of a few millimetres
400 or less.

3.2. Seasonal cycle

401 The mean seasonal cycle, calculated as the mean over the period 2003-2007 for each
402 month, is plotted in fig. 11. In general, a good agreement is found between GRACE and
403 ALMIP seasonal water storage variations for both West Africa and the Sahel. To better
404 compare GRACE estimates and ALMIP output over the Sahel, the water in the Niger
405 River and Niger delta has been removed from the GRACE signal and also plotted (gray
406 curve in fig. 11, right panel): GRACE water storage amplitudes are slightly reduced in
407 September and October but the shape of the seasonal cycle is not substantially changed,
408 in line with the conclusions by *Kim et al.* [2009] for semiarid areas. Correcting for
409 leakage effects, as discussed in section 2.1.1, may further reduce GRACE amplitudes over
410 the Sahel and make them more consistent with ALMIP amplitudes. Mean total run-off by
411 ALMIP (also shown in fig. 11) is between 0 and 15 mm, so the effects of its redistribution
412 on water storage amplitudes cannot be higher than 15 mm. Also ALMIP models do not

413 explicitly account for water table that could increase the water storage amplitudes. Given
414 that, over the Sahel, seasonal water storage amplitudes by GRACE and ALMIP are of
415 the same order, groundwater level variations, not represented in land surface models, do
416 not seem to be the most significant factor affecting water stock variations in this region.

417 Instead, for the West Africa box, GRACE amplitudes may be underestimated because of
418 leakage effects which could therefore enhance the difference between GRACE and ALMIP.
419 This suggests a more important role of slow reservoirs (rivers, dams, aquifers) in the
420 southern part of the study region.

421 Regarding the shape of the seasonal cycle, a steeper slope is observed for GRACE than
422 for ALMIP during the drying-up phase (January to April) for both the West Africa and
423 the Sahel boxes. Only two models ISBA and CLSM (fig. 12 top) show a depletion of
424 available moisture comparable to GRACE results in the Sahel. As shown in Fig. 12
425 (middle) this is mainly due to differences in the formulation of dry season evaporation
426 Indeed for ISBA and CLSM, evapotranspiration during the dry season over the Sahel is
427 about double than for the other ALMIP models (for example, average values between
428 January and April are of 14mm/month for ISBA and 12 mm/month for CLSM). In the
429 case of ISBA, the bare soil parametrisation includes water vapour transfer in addition to
430 liquid water transfer allowing a more efficient drying of the surface layer that may therefore
431 enhance evaporation during the dry season. For the CLSM model, the representation of
432 a saturated zone and of sub grid heterogeneity, redistributing water within the pixel in
433 ponds, shallow water table and temporary flooded areas, results in a longer water retention
434 in the soil layer after the wet season, which allows a sustained evaporation during the dry

435 phases. This longer "memory effect" in the water budget of the CLSM has already been
436 reported by *Mahanama and Koster* [2003].

437 As far as the wet season is concerned (see also fig. 7), soil moisture differences among
438 different models are linked to differences in evapotranspiration for the majority of the
439 models considered here (ISBA, JULES, SWAP, ORCHIDEE, CLSM, SETHYS) for which
440 slightly higher soil moisture values in the wet season correspond to lower evapotranspira-
441 tion, which is related to reduced net radiation (not shown). SSIB and NOAH soil moisture
442 anomalies are less related to evapotraspiration: indeed these two models generate much
443 more total run-off than the land surface model average. In contrast, HTESSEL generates
444 a smaller amount of total run-off than the other models. For HTESSEL and SSIB, these
445 differences can be due to the use of a different soil and vegetation parameters than the
446 other ALMIP models (which used ECOCLIMAP: see Table 2). For NOAH, the high total
447 run-off is likely due to the particular scheme developed by *Decharme* [2007]. Indeed,
448 significant differences in the water budget components are found for models employing
449 the same soil and vegetation parameters. These differences are therefore related to the
450 intrinsic physics of each model and particularly the run-off scheme. CLSM stands apart
451 from the other models, and shows a shift in the seasonal evolution of evapotranspiration
452 that is more delayed into the season with a maximum arriving about one month after the
453 other models which is related to the long memory effect discussed above. It should be
454 noted that the inter-model scatter in the ALMIP models is consistent with other similar
455 off-line model intercomparison projects (see a recent example by *Dirmeyer et al.* [2006])

456 In terms of the seasonal cycle phase, GRACE wetting and drying up periods are gener-
457 ally delayed in comparison to ALMIP results. A similar shift of about one month has been

458 also reported by *Schmidt et al.* [2008], who compared GRACE and models estimations
459 over 18 drainage basins in the world, and was attributed to the incomplete description
460 of water lateral transfers in the water storage modelling. The inclusion of a slow reser-
461 voir, accounting for processes such as surface run-off routing and drainage into deeper
462 soil layers, could change the shape of the seasonal cycle, with more water being retained
463 after the wet season and being evacuated progressively during the dry season, instead of
464 being immediately lost by run-off and drainage. However *Winsemius et al.* [2006] and
465 *Klokocnik* [2008] also found temporal shifts and hypothesize that these could be caused
466 by leakage or the irregular sampling of the GRACE satellites.

3.3. Zonal distribution of land water storage

467 Fig. 13 shows the zonal distribution of soil water storage amplitudes which have been
468 calculated as the difference between the maximum and the minimum values for each
469 latitudinal band for the different GRACE products and the different ALMIP models in
470 2006. The absolute values of the amplitudes vary among GRACE products, but the shape
471 of their zonal distribution is quite similar for all the products with a well defined peak
472 at about 10° N (except for the GFSC solution, which spatial resolution of 4°x4° is not
473 fine enough to determine the shape of the zonal curve). A more important spread in the
474 absolute values of the amplitudes is observed for the ALMIP results, with CLSM much
475 higher and SSIB much lower than the average. Moreover, model outputs do not agree
476 on the shape of the latitudinal distribution with peaks scattered between 8° and 11° N.
477 These differences seem to be at least partially explained by evapotranspiration differences
478 during the dry season. As shown in Fig. 14, models with higher evapotranspiration
479 between December and March correspond to models with the higher soil moisture seasonal

480 amplitudes and vice versa. CLSM exhibits again a distinct behaviour (fig. 13 and 14),
481 which is consistent with its formulation as it is the only LSM including a water table and
482 the effect of deep soil moisture memory. However Gascoïn et al. (2009) showed that this
483 water table may be insufficient to capture large regional aquifer dynamics.

484 We already discussed the role of evapotranspiration during the dry season to explain
485 the soil moisture seasonal curve over the Sahel (fig. 9 right panel). The results reported
486 here show that dry season evapotranspiration plays an important role to the South of the
487 study region also (figs. 13 and 14).

3.4. Interannual variability

488 Interannual variability has been evaluated by subtracting the mean seasonal cycle
489 (shown in Fig. 9) from the water storage temporal evolution in Fig. 7. The results
490 are shown in Fig.15 for the Sahel box. For clarity, the wet season (August-November) and
491 the rest of the year (December to July) are reported separately. From August to Novem-
492 ber, a promising good agreement is found between GRACE and ALMIP: both clearly
493 show, for example, the wet conditions at the end of the 2003 rainy season that was rather
494 good in term of precipitation amount, the important and dramatic drought that affected
495 the Sahel at the end of 2004, the early onset of the monsoon in 2005 and the delayed
496 onset in 2007 and 2006. Similar results (not shown) have been found for the entire West
497 African region. In the December to July period, ALMIP models do not show a significant
498 interannual variability except for a small signature from the previous wet season evident
499 at the end of 2003 and of 2004, which are the extreme wet and dry years. This is may
500 be due to the fact that the ALMIP simulations, except for the CLSM model, do not have
501 strong dynamics in the soil layer below the root zone. On the contrary GRACE estimates

502 indicate large interannual water storage variations for the December to July period also.
503 This could be due to variability in slow water reservoirs that are not well accounted for
504 by models. Even if noise in the GRACE water height solutions may affect the results, the
505 GRACE interannual signature during the dry season is consistent with precipitation in
506 the previous rainy season. GRACE data provide therefore a base to study memory effects
507 and particularly the impact of the previous monsoon season on the following monsoon
508 onset.

4. Concluding discussion

509 The results of this study show that GRACE products provide useful detection of water
510 storage changes over West Africa and the Sahel. An important outcome of this study is
511 that GRACE data are able to reproduce the water storage interannual variability over
512 the Sahel. This is encouraging for the evaluation of water storage monitoring and trend
513 detection, which will be possible when satellite gravimetry data will be available over a
514 sufficiently long time period.

515 Substantial uncertainties remain in terms of the magnitudes estimated by the different
516 GRACE products. The effects of leakage on the estimated water storage variations by
517 GRACE could account for a part of the observed discrepancies, but they should not sub-
518 stantially change the results presented here, at least over the Sahel. Indeed, for the large
519 domains used in this study, the differences among different GRACE solutions, accounted
520 for by the multi-product analysis carried out here, are higher than the estimated effects
521 of leakage .

522 The comparison between GRACE products and ALMIP soil moisture estimations al-
523 lowed the identification of the most critical processes that need to be taken into account

524 to improve water storage modelling over the study area. In line with the findings of other
525 studies comparing GRACE products and land surface model outputs over different areas
526 [*Ngo-Duc et al.* , 2007; *Niu et al.* , 2007; *Güntner et al.* , 2008; *Syed et al.* , 2008; *Kim*
527 *et al.* , 2009; *Alkama et al.* , 2009], the inclusion of slow water reservoirs and transfer
528 schemes routing total run-off in the land surface models could improve the agreement
529 between satellite and model estimates in West Africa. Moreover, we have shown that dry
530 season processes, in particular evapotranspiration, play an important role in the modelling
531 of soil moisture over the Sahel. This is also the case in the Southern part of the study
532 region where vegetation effects are more important. Even when using the same soil and
533 vegetation input data (soil type, soil depth, vegetation type and root depth), models differ
534 in the soil moisture estimations. The simulation of the dynamics of the deepest soil layers
535 is therefore a critical issue, particularly concerning processes related to vertical transfers
536 upwards and downwards, horizontal heterogeneity, transpiration through deep roots and
537 gas phase transfers for dry soil evaporation. This further points out the value of GRACE
538 satellite data for water cycle related studies in this region where observations are quite
539 scarce and modelling is difficult.

5. Appendix

540 Monthly Niger height levels averaged over 2002-2007 have been derived from altimetry
541 data at twelve locations in the Sahel box (Table 4). For each station, river width at the
542 minimum and maximum river height has been derived from Landsat and Google Earth
543 imagery and the River cross section for each monthly data has been estimated assuming
544 a trapezoidal section. The length of the river corresponding to each location (which
545 characteristics are summarised in Table 4) has been derived from Google Earth imagery,

546 excluding the delta (Kirango to Dire). The total length of the Niger river in the Sahel
 547 box is 1636 km (delta excluded).

The water budget of the delta can be written as:

$$\frac{\Delta D}{\Delta t} = F_{in} - F_{out} - ETR_{delta} + (R_{local} + P_{local} + I)$$

548 where D is the mass of water, F_{in} is the water entering the delta measured at
 549 Kirango and Douna and exiting the delta at Dire (data obtained from from GRDC
 550 <http://www.grdc.sr.unh.edu/>), ETR_{delta} represents evaporation losses in the delta. The
 551 other terms are precipitation on the delta (P_{local}), small range run-off contributing to
 552 the delta (R_{local}) and exchanges with water tables (I), which are neglected ([*Mahé et al.*
 553 , 2009]). ETR_{delta} is computed as the product of the flood surface S_{delta} by monthly
 554 evaporation rate for open water E given by *Quensière et al.* [1994], table 5, as:

$$ETR_{delta} = E \cdot S_{delta}$$

555 The flooded surface is estimated for 2003 using equations given by *Zwart and Grigoras*
 556 [2005] for expanding and receding periods, based on water height data at Akka and landsat
 557 images.

558 To ensure consistency, monthly ETR for 2003 has been rescaled so that annual ETR
 559 corresponds to annual $F_{in} - F_{out}$ which is measured over 1922-1992.

560 **Acknowledgments.**

561 First of all, the authors deeply acknowledge all the participants to the ALMIP Working
 562 Group (A. Boone, P. de Rosnay, G. Balsamo, A. Beljaars, F. Chopin, B. Decharme, C.
 563 Delire, A. Ducharne, S. Gascoin, M. Grippa, F. Guichard, Y. Gusev, P. Harris, L. Jarlan,
 564 L. Kergoat, E. Mougin, O. Nasonova, A. Norgaard, T. Orgeval, C. Ottlé, I. Pocard-

565 Leclercq, J. Polcher, I. Sandholt, S. Saux-Picart, C. Taylor): without their effort on the
566 ALMIP project this study would not have been possible.

567 Many thanks to Anny Cazenave and Ines Fung for useful discussions about GRACE
568 and to Luc Seguis for providing his expertise and feedback on the hydrology of Soudanian
569 West African region. We also acknowledge Laurent Longuevergne and three anonymous
570 reviewers that carefully read the first version of this manuscript and provided useful
571 comments by which the final manuscript was largely improved.

572 This work was undertaken under the AMMA project. Based on a French initiative,
573 AMMA was built by an international scientific group and is currently funded by a large
574 number of agencies, especially from France, the UK, the USA and Africa. It has been
575 the beneficiary of a major financial contribution from the European Communitys Sixth
576 Framework Research Programme. F. Frappart was funded by a CNRS post-doctoral
577 grant.

578 GRACE CSR, JPL and GFZ data were processed by D. P. Chambers, supported by
579 the NASA Earth Science REASoN GRACE Project. Altimetry data have been provided
580 by J. F. Cretaux.

References

- 581 Alkama, R., B. Decharme, H. Douville, M. Becker, A. Cazenave, J. Sheffield, A. Voltaire,
582 S. Tyteca and P. Le Moigne (2009), Global evaluation of the ISBA-TRIP continental
583 1 hydrologic system, Part 1: A twofold constraint using GRACE Terrestrial Water
584 Storage estimates and in-situ river discharges, *J. Hydromet.*, under revision.
- 585 Andersen O. B., S. I. Seneviratne, J. Hinderer and P. Viterbo (2005), GRACE-derived ter-
586 restrial water storage depletion associated with the 2003 European heat wave, *Geophys.*

- 587 *Res. Lett.*, *32*, 18, L18405.
- 588 Balsamo, G., P. Viterbo, A. Beljaars, B. van den Hurk, M. Hirsch, A. Betts, and K.
589 Scipal (2009), A revised hydrology for the ECMWF model: Verification from field site to
590 terrestrial water storage and impact in the Integrated Forecast System, *J. Hydrometeor.*,
591 *10*, 623643.
- 592 Boone, A., P. de Rosnay, G. Balsamo, A. Beljaars, F. Chopin, B. Decharme, C. Delire, A.
593 Ducharne, S. Gascoin, M. Grippa, F. Guichard, Y. Gusev, P. Harris, L. Jarlan, L. Ker-
594 goat, E. Mougin, O. Nasonova, A. Norgaard, T. Orgeval, C. Ottl, I. Pocard-Leclercq, J.
595 Polcher, I. Sandholt, S. Saux-Picart, C. Taylor (2009), The AMMA Land Surface Model
596 Intercomparison Project (ALMIP), *Bulletin American Meterological Society*, *90(12)*,
597 1865-1880.
- 598 Braud I., P. Bessemoulinb, B Montenyc, M Sicot, J.P. Vandervaerea, M. J Vauclina (1997),
599 Unidimensional modelling of a fallow savannah during the HAPEX-Sahel experiment
600 using the SiSPAT model, *J. Hydrol.*, *188-189*, 912-943.
- 601 Bruinsma S., Lemoine J-M., Biancale R., Valls N. (2010), CNES/GRGS 10-day gravity
602 field models (release 2) and their evaluation, *Advances in Space Research*, *45*, 587601.
- 603 Chambers, D. P. (2006), Evaluation of new GRACE time-variable gravity data over the
604 ocean, *Geophys. Res. Lett.*, *33(17)*, L17603.
- 605 Chen, F., and J. Dudhia (2001), Coupling an advanced land surface-hydrology model
606 with the Penn State-NCAR MM5 modelling system. Part I: Model implementation and
607 sensitivity, *Mon. Wea. Rev.*, *129*, 569-585.
- 608 Chen, J. L., C.R. Wilson, J. S. Famiglietti and M. Rodell (2005), Spatial sensitivity of
609 the Gravity Recovery and Climate Experiment (GRACE) time-variable gravity obser-

- 610 vations, *J. Geophys. Res.*, *110*, B08408, doi:10.1029/2004JB003536.
- 611 Chen, J.L., C.R. Wilson, B.D. Tapley, Z.L. Wang and G.Y. Niu (2009), 2005 drought event
612 in the Amazon River basin measured by GRACE and estimate by climate models, *J.*
613 *Geophys. Res.*, *114*, doi:10.1029/2008JB006056.
- 614 Crowley, J.W. , J.X. Mitrovica, R.C. Bailey, M.E. Tamisiea and J.L. Davis (2006), Land
615 water storage within the Congo Basin inferred from GRACE satellite gravity data,
616 *Geophys. Res. Lett.*, *33(19)*, L19402
- 617 Decharme, B. (2007), Influence of the runoff representation on continental hydrology
618 using the NOAH and the ISBA land surface models. *J Geophys Res*, *112*, D19108,
619 doi:10.1029/2007JD008463.
- 620 Descroix L., G. Mah, T. Lebel, G. Favreau, S. Galle, E. Gautier, J.-C. Olivry, J. Albergel,
621 O. Amogu, B. Cappelaere, R. Dessouassi, A. Diedhou, E Le Breton, I. Mamadou,
622 D. Sighomnou (2009), Spatio-temporal variability of hydrological regimes around the
623 boundaries between Sahelian and Sudanian areas of West Africa : A synthesis, *J. Hy-*
624 *drol.*, *375*, 90-102
- 625 Dirmeyer, P. A., X. Gao, M. Zhao, Z. Guo, T. Oki, and N. Hanasaki (2006), GSWP-2:
626 Multi-model Analysis and Implications for Our Perception of the Land Surface, *Bull.*
627 *Amer. Meteor. Soc.*, *87*, 1381-1397.
- 628 Ditmar,P., R. Klees, and X. Liu (2007), Frequency-dependent data weighting in global
629 gravity field modeling from satellite data contaminated by non-stationary noise, *Journal*
630 *of Geodesy*, *81*, 8196.
- 631 Essery, R. L. H., M. Best, R. Betts, P. Cox, and C. M. Taylor (2003), Explicit repre-
632 sentation of subgrid heterogeneity in a GCM land surface scheme, *J Hydrometeor*, *4*,

- 633 530-543.
- 634 Favreau, G., B. Cappelaere, S. Massuel, M. Leblanc, M. Boucher, N. Boulain,
635 and C. Leduc (2009), Land clearing, climate variability, and water resources in-
636 crease in semiarid southwest Niger: A review, *Water Resour. Res.*, *45*, W00A16,
637 doi:10.1029/2007WR006785.
- 638 Frappart, F., G. Ramillien, M. Leblanc, S.O. Tweed, M.-P. Bonnet and P. Maisongrande
639 (2011), An independent component analysis filtering approach for estimating continental
640 hydrology in the GRAE gravity data, *Rem. Sens. Environ.*, *115*, 187-204
- 641 Gascoin, S. (2009), Etude des paramétrisations hydrologiques dun modèle de surface con-
642 tinentale : importance des aquifères et des premiers centimètres du sol, *Doctoral thesis*,
643 available at <http://tel.archives-ouvertes.fr/>
- 644 Giannini, A., R. Saravanan and P. Chang (2003), Oceanic forcing of Sahel rainfall on
645 interannual to interdecadal time scales, *Science*, *302*, 5647, 1027-1030.
- 646 Giannini A., M. Biasutti and M.M. Verstraete (2008), A climate model-based review of
647 drought in the Sahel: Desertification, the re-greening and climate change, *Global Plan.*
648 *Change*, *64(3-4)*, 119-128.
- 649 Güntner, A. (2008), Improvement of global hydrological models using GRACE data, *Surv.*
650 *Geophys.*, *29*, 375397.
- 651 Gusev, E. M., O. N. Nasonova and E. E. Kovalev (2006), Modeling the components of
652 heat and water balance for the land surface of the globe, *Water Resour*, *33*, 616-627.
- 653 Huffman, G. J., R. F. Adler, D. T. Bolvin, G. Gu, E. J. Nelkin, K. P. Bowman, Y. Hong,
654 E. F. Stocker and D. B. Wolff (2007), The TRMM Multi-satellite Precipitation Analysis:
655 Quasi-Global, Multi-Year, Combined-Sensor Precipitation Estimates at Fine Scale, *J.*

- 656 *Hydromet.*, 8, 38-55.
- 657 Kim, H., P. J.-F. Yeh, T. Oki, and S. Kanae (2009), Role of rivers in the seasonal vari-
658 ations of terrestrial water storage over global basins, *Geophys. Res. Lett.*, 36, L17402,
659 doi:10.1029/2009GL039006.
- 660 Klees, R., E. A. Zapreeva, H. C. Winsemius, and H. H. G. Savenije (2007), The bias in
661 GRACE estimates of continental water storage variations. *Hydrol. Earth Syst. Sci.*, 11,
662 1227-1241.
- 663 Klees, R., X. Liu, T. Wittwer, B. C. Günter, E. A. Revtova, R. Tenzer, P. Ditmar, H.
664 C. Winsemius and H. H. G. Savenije (2008), A Comparison of Global and Regional
665 GRACE Models for Land Hydrology, *Surv. Geophys.*, 29, 335-359.
- 666 Klees, R., E. A. Rervtova, B. Günter, P. Ditmar, E. Oudman, H. C. Winsemius, and H. H.
667 Savenije (2008), The design of an optimal filter for monthly grace gravity field models,
668 *Geophysical Journal International*, 175, 417432.
- 669 Koster, R.D., M. J. Suarez, A. Ducharne, P. Kumar and M. Stieglitz (2000), A catchment-
670 based approach to modeling land surface processes in a GCM - Part 1: Model structure,
671 *J Geophys Res*, 105, 24809-24822.
- 672 Koster R. D., P. A. Dirmeyer, Z. Guo, G. Bonan, E. Chan, P. Cox, C. T. Gordon, S.
673 Kanae, E. Kowalczyk, D. Lawrence, P. Liu, C.-H. Lu, S. Malyshev, B. McAvaney,
674 K. Mitchell, D. Mocko, T. Oki, K. Oleson, A. Pitman, Y. C. Sud, C. M. Taylor, D.
675 Verseghy, R. Vasic, Y. Xue and T. Yamada (2004), Regions of strong coupling between
676 soil moisture and precipitation, *Science*, 305, 1138-1140.
- 677 Klokocnik, J., C. A. Wagner, J. Kostelecký, A. Bezděk, P. Novák, and D. McAdoo (2008),
678 Variations in the accuracy of gravity recovery due to ground track variability: GRACE,

- 679 CHAMP, and GOCE, *J. Geod.*, *82*, 917-927.
- 680 Klosko, S., D. Rowlands, S. Luthcke, F. Lemoine, D. Chinn and M. Rodell (2009), Eval-
681 uation and validation of mascon recovery using GRACE KBRR data with independent
682 mass flux estimates in the Mississippi Basin, *J. Geodesy*, *83(9)*, 817-827.
- 683 Kusche, J., (2007), Approximate decorrelation and non-isotropic smoothing of time-
684 variable GRACE-type gravity fields, *Journal of Geodesy*, *81*, 733-749.
- 685 Lebel, T., J.D. Taupin, and N. d'Amato (1997), Rainfall monitoring during HAPEX-
686 Sahel: 1. General rainfall conditions and climatology. *Journal of Hydrology*, *188-189*,
687 74-96.
- 688 Liu, X., (2008), Global gravity field recovery from satellite-to-satellite tracking data with
689 the acceleration approach (Ph. D. Thesis), *Nederlands Geodetic Comission, Publications*
690 *on Geodesy*, *68*, Delft, The Netherlands.
- 691 Llubes, M., J.-M. Lemoine and F. Remy (2007), Antarctica seasonal mass variations
692 detected by GRACE, *Earth Planet Sci Lett*, *260(1-2)*, 127-136.
- 693 Longuevergne L., B. S. Scanlon and C. R. Wilson (2010), GRACE Hydrological estimated
694 for small basins: evaluating processing approaches on the High Plains Aquifer, USA
695 *Wat. Resour. Res.*, *46*, W11517.
- 696 Mahanama S.P.P. and R.D. Koster (2003), Intercomparison of Soil Moisture Memory in
697 Two Land Surface Models, *Journal of Hydrometeorology*, *4*, 1134-1146.
- 698 Mahè G, F. Bamba, A. Soumaguel, D. Orange, and J.-C. Olivry (2009), Water losses in
699 the inner delta of the River Niger: water balance and flooded area, *Hydrol. Process.*,
700 *23*, 31573160. DOI: 10.1002/hyp.7389

- 701 Ngo-Duc, T., K. Laval, G. Ramillien, J. Polcher and A. Cazenave (2007), Validation
702 of the landwater storage simulated by Organising Carbon and Hydrology in Dynamic
703 Ecosystems (ORCHIDEE) with Gravity Recovery and Climate Experiment (GRACE)
704 data, *Water Resour. Res.*, *43*, W04427.
- 705 Niu, G.-Y., Z.-L. Yang, R.E. Dickinson, L.E. Gulden H. and Su (2007), Development
706 of a simple groundwater model for use in climate models and evaluation with Gravity
707 Recovery and Climate Experiment data, *J. Geophys. Res.*, *112*, D07103. 4815- 4817
- 708 Noilhan, J., and J.-F. Mahfouf (1996), The ISBA land surface parameterization scheme,
709 *Global Planet Change*, *13*, 145159.
- 710 d'Orgeval T., J. Polcher and P. de Rosnay (2008), Sensitivity of the West African hydro-
711 logical cycle in ORCHIDEE to infiltration processes, *Hydrol Earth Syst Sci Discuss*, *5*,
712 2251-2292.
- 713 Papa F., A. Guntner, F. Frappart, C. Prigent, W.B. Rossow (2008), Variations of surface
714 water extent and water storage in large river basins: A comparison of different global
715 data sources, *Geophys. Res. Lett.*, *35(11)*, L11401.
- 716 Peugeot, C., M. Esteves, S. Galle, J.L. Rajot and J.P. Vandervaere (1997), Runoff gener-
717 ation processes: Results and analysis of field data collected at the east central supersite
718 of the HAPEX-Sahel experiment, *J. Hydrol.*, *189*, 179-202.
- 719 Quensière J, J.C. Olivry, Y. Poncet and J. Wuillot (1994), Environnement deltaïque, *La*
720 *peche dans le delta central du Niger: approche pluridisciplinaire dun systeme de produc-*
721 *tion halieutique*, *Quensiere J. (ed.)*, ORSTOM-Karthala, Paris, pp 43-77.
- 722 Philippon, N., and B. Fontaine (2002), The relationship between the Sahelian and previ-
723 ous 2nd Guinean rainy seasons: a monsoon regulation by soil wetness?, *Ann. Geophys.*,

724 20, 575-582.

725 Ramillien G., F. Frappart, A. Cazenave and A. Guntner (2005), Time variations of land
726 water storage from an inversion of 2 years of GRACE geoids, *Earth Planet. Sci. Lett.*,
727 *253(1-2)*, 283-301.

728 Ramillien, G., F. Frappart, A. Guntner, T. Ngo-Duc, A. Cazenave and K. Laval (2006),
729 Time variations of the regional evapotranspiration rate from Gravity Recovery and Cli-
730 mate Experiment (GRACE) satellite gravimetry, *Wat. Resour. Res.*, *42(10)*, W10403.

731 Ramillien, G. , J.S. Famiglietti and J. Wahr (2008), Detection of Continental Hydrology
732 and Glaciology Signals from GRACE: A Review, *Surv. Geophys.*, *29(4-5)*, 361-374.

733 Ramillien, G., S. Bouhours, A. Lombard, A. Cazenave, F. Flechtner and R. Schmidt
734 (2008), Land water storage contribution to sea level from GRACE geoid data over
735 2003-2006, *Global Planetary Change*, *60(3-4)*, 381-392.

736 Rodell, M., J.S. Famiglietti, J. Chen, S.I. Seneviratne, P. Viterbo, S. Holl and C.R.
737 Wilson (2004), Basin scale estimates of evapotranspiration using GRACE and other
738 observations, *Geophys. Res. Lett.*, *31*, 20, L20504.

739 de Rosnay, P., J. Polcher, M. Bruen and K. Laval (2002), Impact of a physically based
740 soil water flow and soil-plant interaction representation for modeling large scale land
741 surface processes., *J. Geophys. Res.*, *107(D11)*, 4118, doi:10.1029/2001JD000634.

742 Rowlands, D.D., S.B. Luthcke, S.M. Klosko, F.G.R. Lemoine, D.S. Chinn, J.J. McCarthy,
743 C.M. Cox and O.B. Anderson (2005), Resolving mass flux at high spatial and tempo-
744 ral resolution using GRACE intersatellite measurements, *Geophys. Res. Lett.*, *32(4)*,
745 L04310.

- 746 Saux-Picart, S., C. Otllé, A. Perrier, B. Decharme, B. Coudert, M. Zribi, N. Boulain, B.
747 Cappelaere, D. Ramier (2009), SEtHyS_Savannah: A multiple source land surface model
748 applied to Sahelian landscapes, *Agricultural and Forest Meteorology*, *149(9)*, 1421-1432.
- 749 Schmidt, R., P. Schwintzer, F. Flechtner, C. Reigber, A. Guntner, P. Doll, G. Ramillien,
750 A. Cazenave, S. Petrovic, H. Jochmann and J. Wunsch (2006), GRACE observations of
751 changes in continental water storage, *Global Planetary Change*, *50(1-2)*, 112-126.
- 752 Schmidt, R., S. Petrovic, A. Guntner, F. Barthelmes, J. Wunsch and J. Kusche (2008), Pe-
753 riodic components of water storage changes from GRACE and global hydrology models,
754 *J. Geophys. Res.- Solid Earth*, *113*, B8, B08419.
- 755 Seitz, F., M. Schmidt and C.K. Shum (2008), Signals of extreme weather conditions in
756 Central Europe in GRACE 4-D hydrological mass variations, *Earth Planet. Science*
757 *Lett.*, *268(1-2)*, 165-170.
- 758 Sultan, B., and S. Janicot (2003), The West African monsoon dynamics. Part II: The
759 'preonset' and 'onset' of the summer monsoon, *J. Clim.*, *16(21)*, 3407-3427.
- 760 Swenson, S., and J. Wahr (2006), Estimating large-scale precipitation minus evapotran-
761 spiration from GRACE satellite gravity measurements, *J. Hydromet.*, *7(2)*, 252-270.
- 762 Swenson, S., and J. Wahr (2006), Post-processing removal of correlated errors in GRACE
763 data, *Geophys. Res. Lett.*, *33*, L08402, doi:10.1029/2005GL025285.
- 764 Swenson, S., J.S. Famiglietti, J. Basara and J. Wahr (2008), Estimating profile soil mois-
765 ture and groundwater variations using GRACE and Oklahoma Mesonet soil moisture
766 data, *Water. Res. Res.*, *44(1)*, W01413.
- 767 Syed, T.H., J.S. Famiglietti, J. Chen, M. Rodell, S.I. Seneviratne, P. Viterbo and C.R.
768 Wilson (2005), Total basin discharge for the Amazon and Mississippi River basins from

- 769 GRACE and a land-atmosphere water balance, *Geophys. Res. Lett.*, *32*(24), L24404.
- 770 Syed, T.H. , J.S. Famiglietti, M. Rodell, J. Chen and C.R. Wilson (2008), Analysis of
771 terrestrial water storage changes from GRACE and GLDAS, *Water. Res. Res.*, *44*(2),
772 W02433.
- 773 Winsemius, H. C., H. H. G. Savenije, N. C. Van de Giesen, B. J. J. M. Van den Hurk, E. A.
774 Zapreeva, and R. Klees, 2006, Assessment of Gravity Recovery and Climate Experiment
775 (GRACE) temporal signature over the upper Zambezi. *Wat. Resour. Res.*, *42*, W12201.
- 776 Xue, Y., P. J. Sellers, J. L. Kinter and J. Shukla (1991), A simplified biosphere model for
777 global climate studies, *J. Climate*, *4*, 345364.
- 778 Yirdaw, S.Z., K.R. Snelgrove and C.O. Agboma (2008), GRACE satellite observations
779 of terrestrial moisture changes for drought characterization in the Canadian Prairie, *J.*
780 *Hydrol.*, *356*(1-2), 84-92.
- 781 Zwarts L., and I. Grigoros, 2005, Flooding of the inner Niger delta, *The Niger, a lifeline.*
782 *Effective water management in the Upper Niger Basin*, Zwarts L., P. van Beukering,
783 E. Kone, E. Wymenga (eds), RIZA, Lelystad / Wetlands International, Svar, / In-
784 stitute for Environmental Studies (IVM), Amsterdam, / A&W ecological consultants,
785 Veenwouden. Mali/ the Netherlands, pp 43-77.

Table 1. GRACE products employed in this study.

Product name	Spatial grid	Spatial resolution	Temporal frequency	Time span
GFZ -v 04	1°x1°	400 km	1 month	Oct 2002-Apr 2008 (missing Jan 2003, Jun 2003, Jan 2004, Sept 2004*)
JPL -v 04	1°x1°	400 km	1 month	Aug 2002-Apr 2008 (missing Jan 2003, Jun 2003, Jan 2004)
CSR -v 4.1	1°x1°	400 km	1 month	Sep 2002-Apr 2008 (missing Jun 2003, Jan 2004)
DEOSS DMT V 1	1°x1°	400 km	1 month	Feb 2003 - Dec 2007 (missing Jun. 2003)
CNES -GRGS v 2	1°x1°	400 km	10 days	Aug 2002-May 2008
GSFC -Mascons	4°x4°	4°x4°	10 days	Apr 2003-Apr 2007

* removed because of aliasing problems

Table 2. Land surface models participating to ALMIP-Exp3. The names of the people who performed the simulations are in *italic* below the institute name. The model configuration used for ALMIP is shown in the rightmost column where L represents the number of vertical soil layers, E represents the number of energy budgets per tile, and SV corresponds to the soil-vegetation parameters used. Tile refers to the maximum number of completely independent land surface types permitted within each grid box.

Model Acronym	Institute	Recent Reference	ALMIP configuration
HTESSEL	ECMWF, Reading, UK <i>G. Balsamo</i>	<i>Balsamo et al.</i> [2008]	4L, 6 tiles, 1E, SV: ECMWF
ORCHIDEE -CWRR	IPSL, Paris, France <i>P. de Rosnay</i>	<i>d'Orgeval et al.</i> [2008]; <i>de Rosnay et al.</i> [2002]	11L, 13 tiles, 1E, SV: ECOCLIMAP
ISBA	CNRM, Toulouse, France <i>A. Boone</i>	<i>Noilhan and Mahfouf</i> [1996]	3L, 1 tile, 1E, SV : ECOCLIMAP
JULES	CEH, Wallingford, UK <i>P. Harris</i>	<i>Essery et al.</i> [2003]	4L, 9 tiles, 2E, SV: ECOCLIMAP
SETHYS	CETP/LSCE, France <i>S. Saux-Picart and C. Ottlé</i>	<i>Saux-Picart et al.</i> [2009]	3L, 12 tiles, 2E, SV: ECOCLIMAP
NOAH	CETP/LSCE (NCEP) <i>B. Decharme and C. Ottlé</i>	<i>Chen and Dudhia</i> [2001]; <i>Decharme</i> [2007]	7L, 12 tiles, 1E, SV: ECOCLIMAP
CLSM	UPMC, Paris, France <i>S. Gascoïn and A. Ducharne</i>	<i>Koster et al.</i> [2000] <i>Gascoïn</i> [2009]	3L, 5 tiles, 1E, SV: ECOCLIMAP
SSiB	LETG, Nantes, France; UCLA, Los Angeles, USA <i>I. Pocard-Leclercq</i>	<i>Xue et al.</i> [1991]	3L, 1 tile, 2E, SV: SSiB
SWAP	IWP, Moscow, Russia <i>Y. Gusev and O. Nasonova</i>	<i>Gusev et al.</i> [2006]	3L, 1 tile, 1E, SV: ECOCLIMAP

Table 3. Water budget components by the ALMIP land surface models over West Africa and the Sahel. For the ensemble of the ALMIP models considered, mean values are reported.

	West Africa				
	2003	2004	2005	2006	2007
Precipitation (mm/year)	894	769	698	740	791
Evaporation (mm/year)	639	619	591	585	575
Surface runoff (mm/year)	67	52	44	49	61
Drainage (mm/year)	164	110	77	103	145
	Sahel				
	2003	2004	2005	2006	2007
Precipitation (mm/year)	535	404	449	433	433
Evaporation (mm/year)	437	362	381	377	361
Surface runoff (mm/year)	35	24	26	23	28
Drainage (mm/year)	58	32	33	29	40

Table 4. Characteristics of the altimetry stations used to estimate water mass in the Niger river in the Sahel box.

Station ID	Lat	Lon	min width (m)	max width (m)	River length (km)
259	13.18	352.89	600	3090	295.0
173	13.72	354.20	300	2400	87.0
459	16.67	357.11	600	2100	23.5
388	16.73	357.44	1000	4000	43.5
917	16.83	357.80	400	1500	49.0
846	16.92	358.20	380	1500	45.5
373	17.01	358.47	500	4500	60.5
302	17.01	358.94	260	1550	58.0
831	17.00	359.19	400	2000	55.0
760	16.94	359.64	500	7000	102.5
287	15.96	0.15	370	2800	183.0
745	14.31	1.25	550	2900	633.5

Table 5. Monthly evaporation rate(mm) after *Quensière et al.* [1994]

Jan	Feb	Mar	Apr	May	Jun	Jul	Aug	Sep	Oct	Nov	Dec
167	187	212	219	230	215	205	170	173	180	180	160

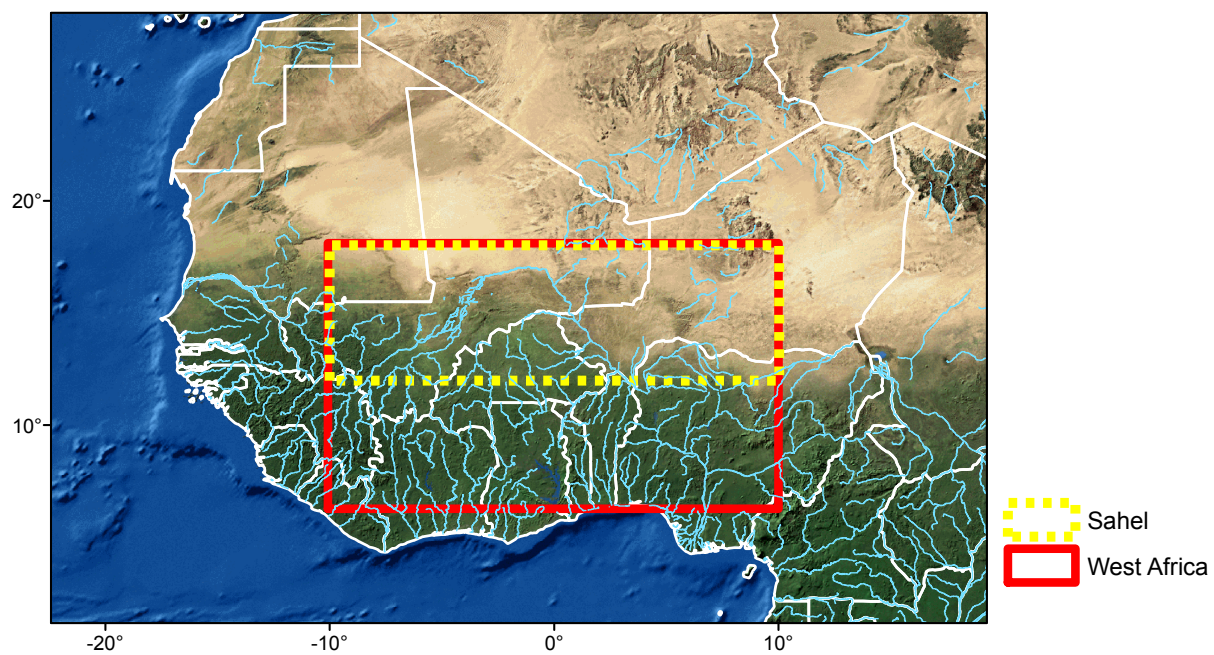


Figure 1. Study area, with overlaid the West Africa and Sahel boxes employed in this study.

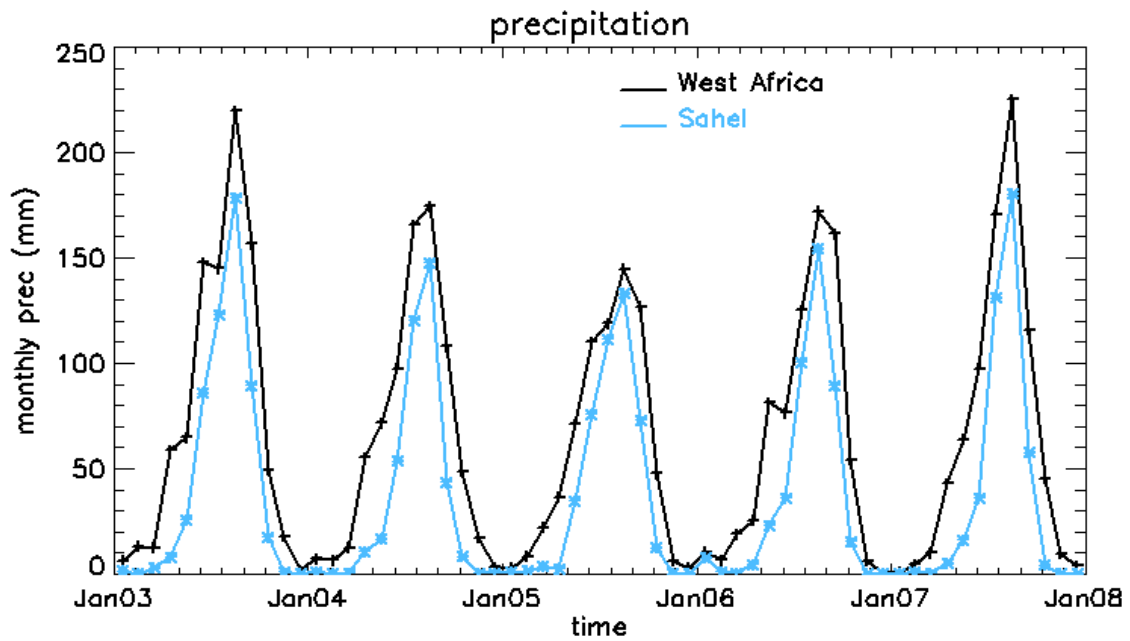


Figure 2. Monthly precipitation (mm) over West Africa and the Sahel by the TRMM dataset employed for the ALMIP simulations.

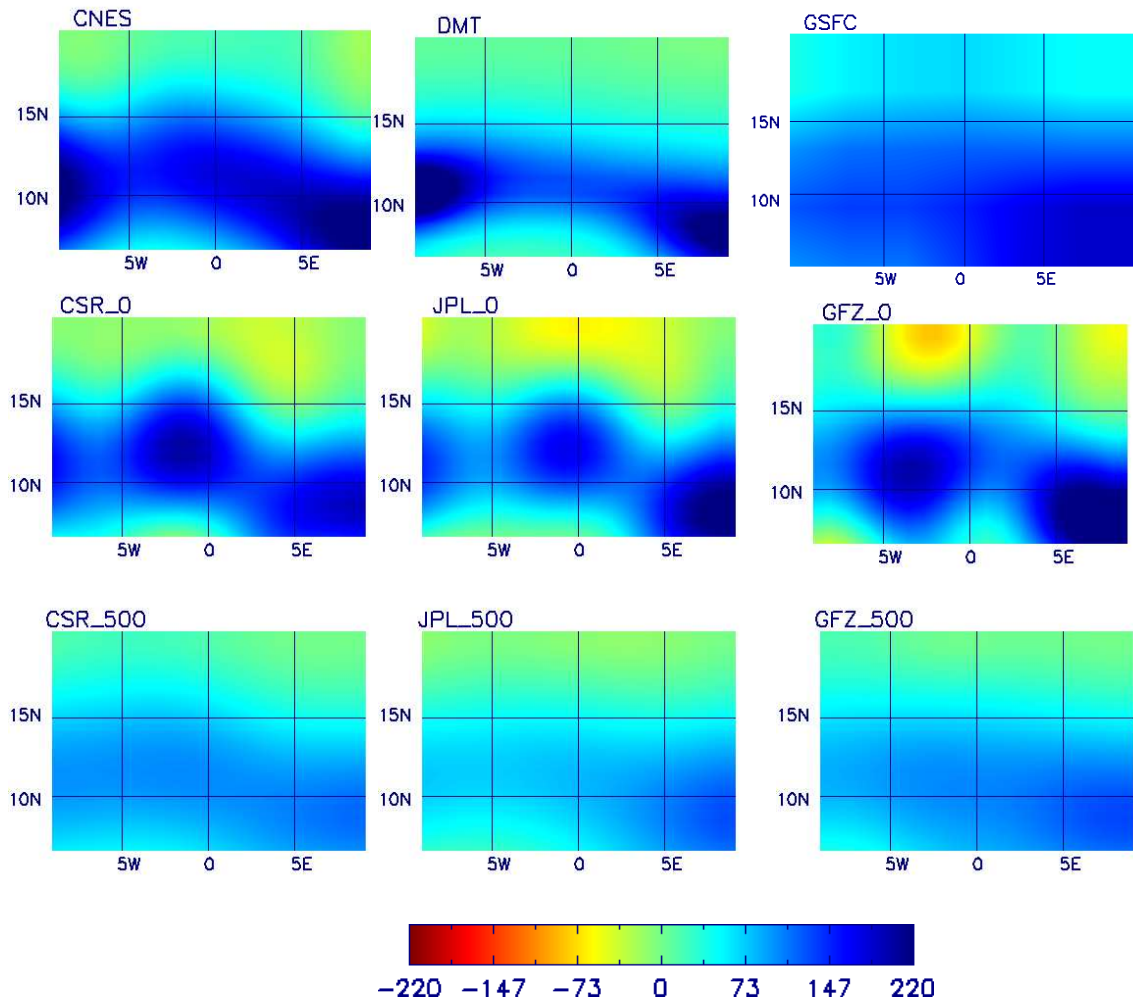


Figure 3. Spatial distribution of water storage anomalies (mm) over the West Africa study region for all the GRACE products. September 2006.

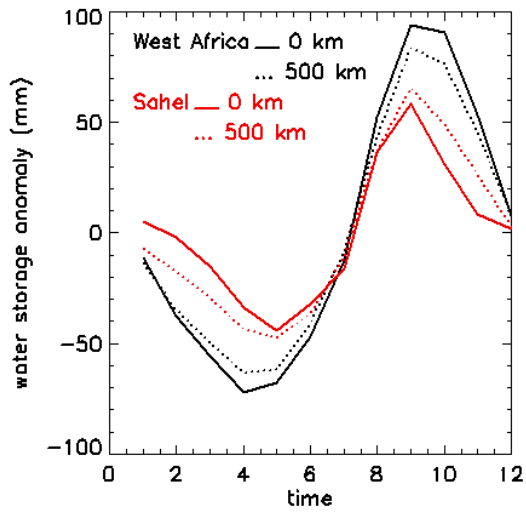


Figure 4. Seasonal cycle (multi annual mean over the study period 2003-2007) for CSR, JPL and GFZ solutions unsmoothed and smoothed by a Gaussian filter of 500 km.

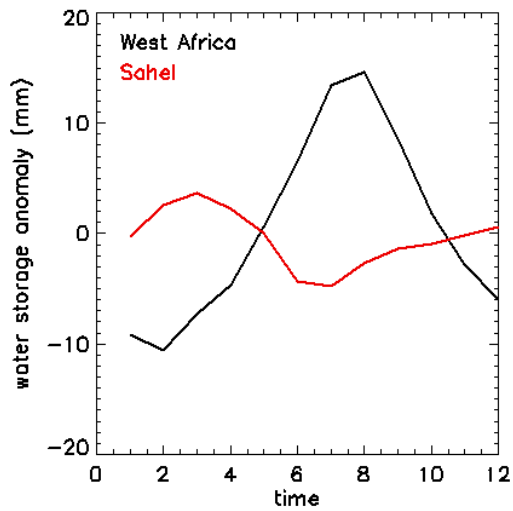


Figure 5. Leakage correction for CSR solutions over West Africa and the Sahel

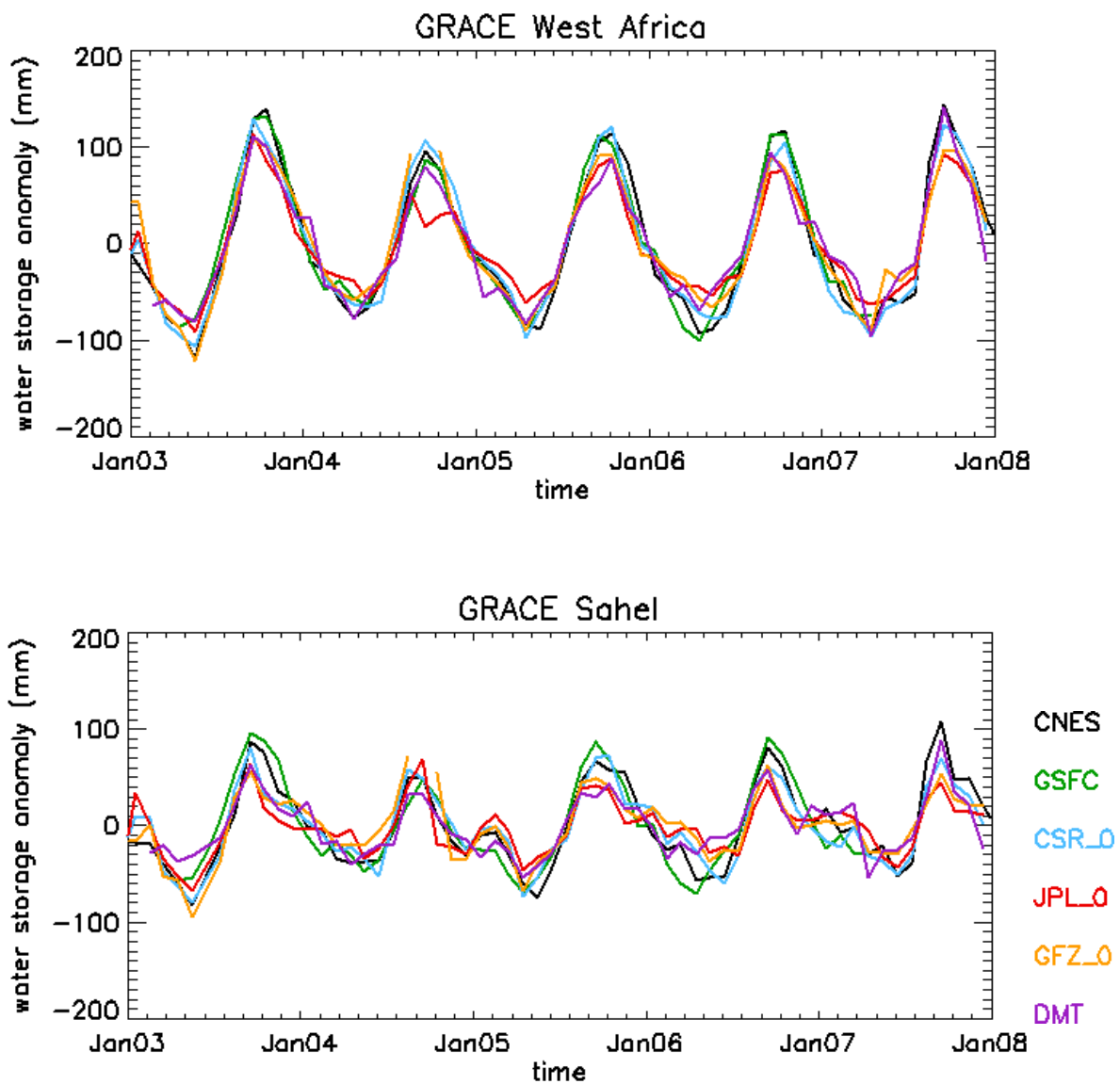


Figure 6. Water storage changes for the 6 different GRACE solutions employed in this study, spatially averaged over the West Africa and the Sahel boxes.

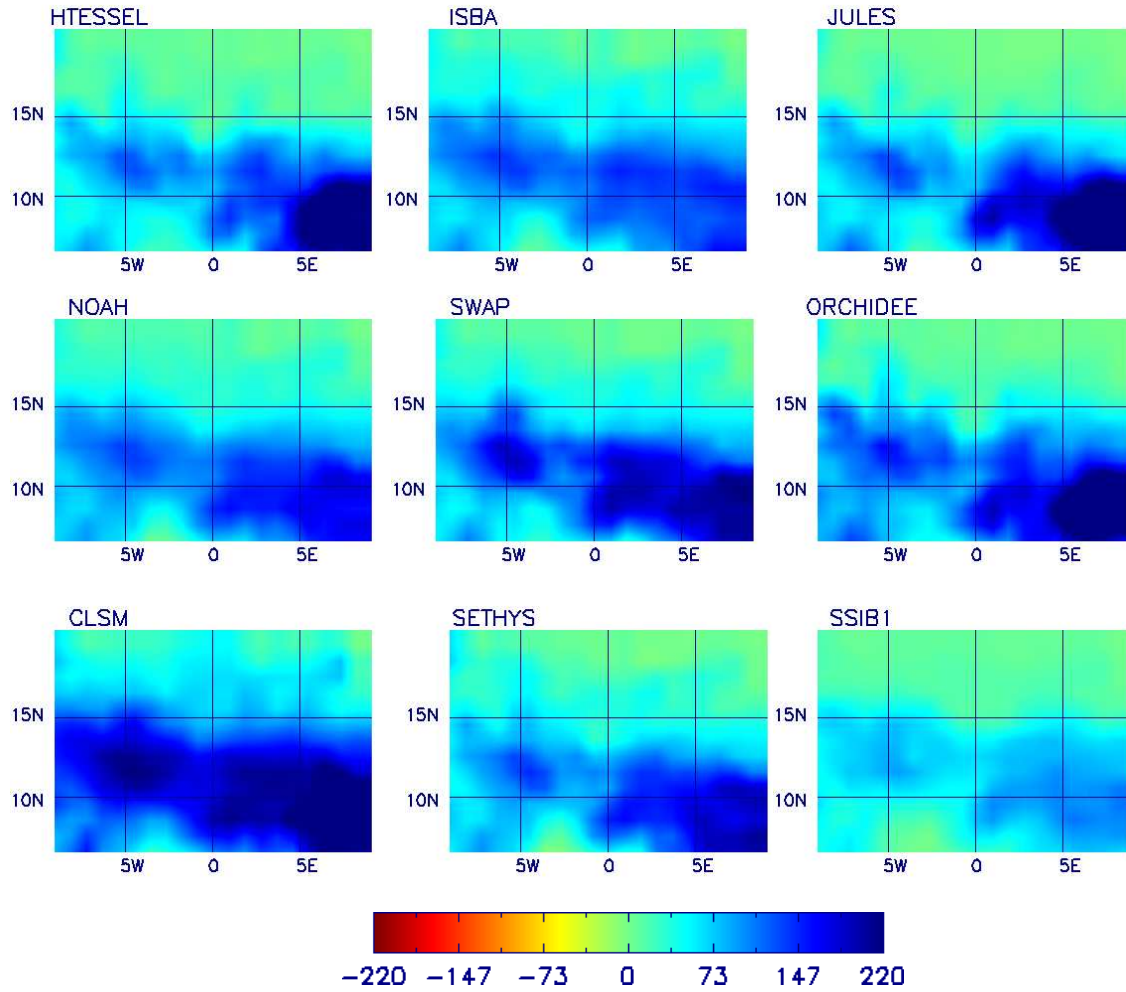


Figure 7. Spatial distribution of water storage anomalies (mm) over the West Africa study region for all the ALMIP models analysed. September 2006.

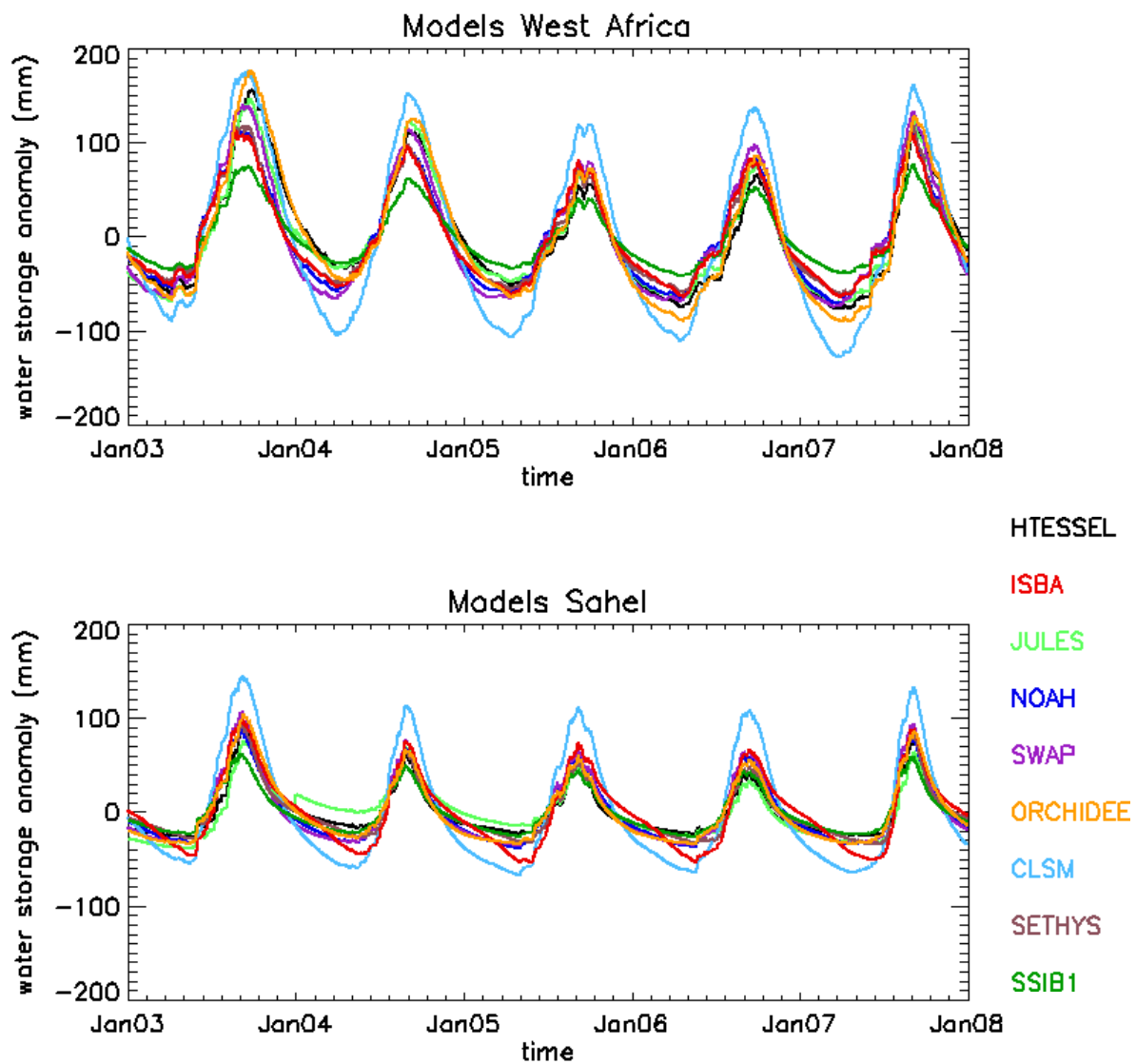


Figure 8. Simulated water storage changes for the 9 different models employed in this study, spatially averaged over the West Africa and the Sahel boxes.

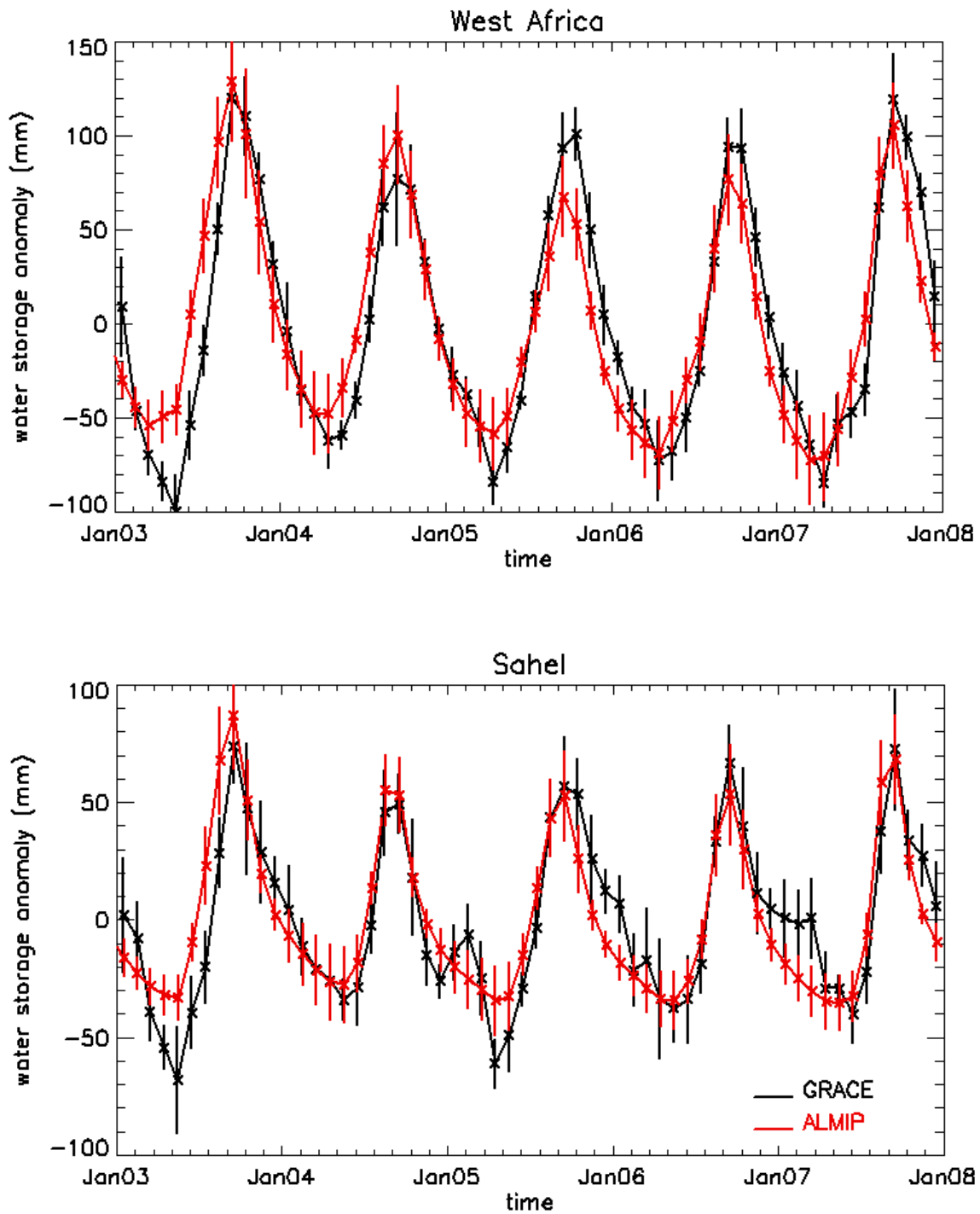


Figure 9. Temporal evolution of GRACE (multi-solutions mean and standard deviation) and ALMIP (multi-models mean and standard deviation) water storage variations for the West Africa and the Sahel.

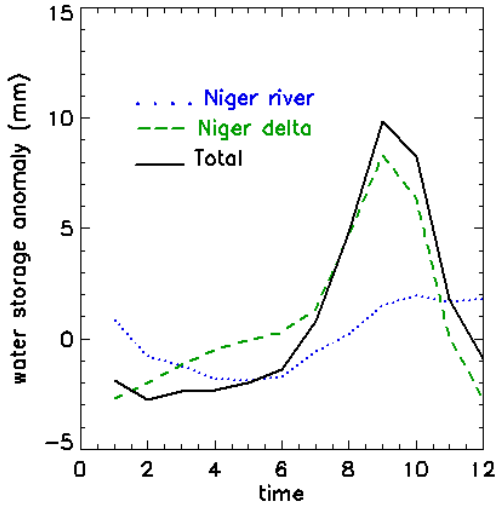


Figure 10. Water storage contribution from the Niger river (water in the river itself, in the delta and total) in the Sahel box.

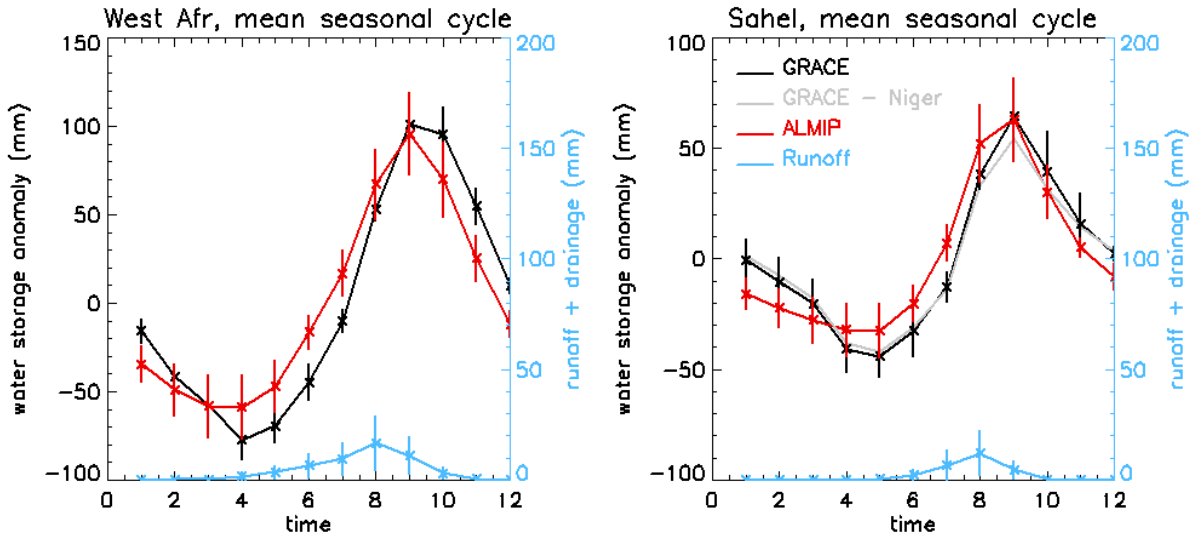


Figure 11. Water storage mean seasonal cycle over the period 2003-2007 for GRACE (multi-solutions mean and standard deviation) and ALMIP (multi-models mean and standard deviation). The mean total run-off by ALMIP is also shown in blue. The Gray curve on the right hand plot represents the GRACE water storage without the Niger river contribution (fig. 10)

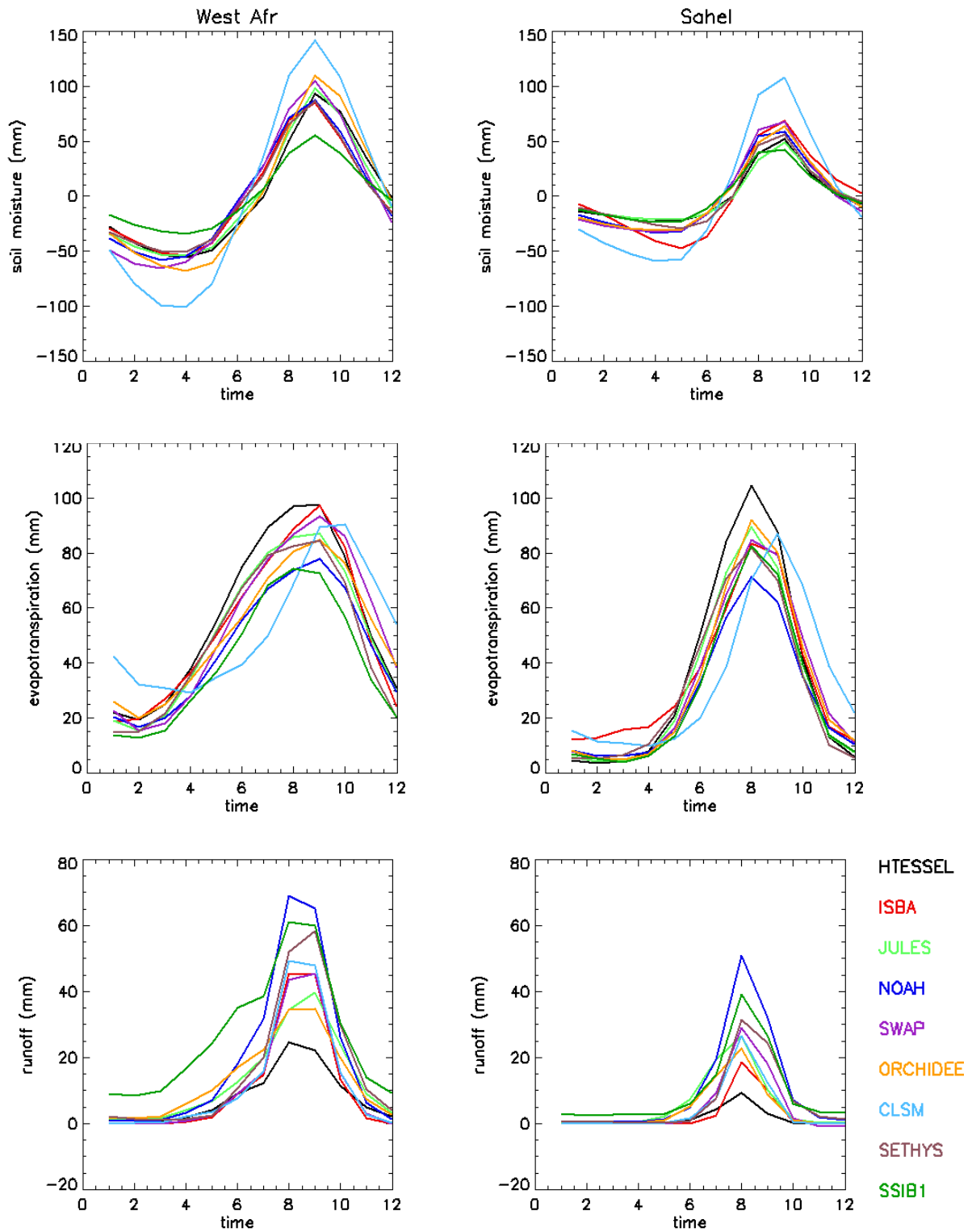


Figure 12. Soil moisture, evaporation and total run-off (runoff+drainage) mean seasonal cycle over the period 2003-2007 for the different ALMIP models.

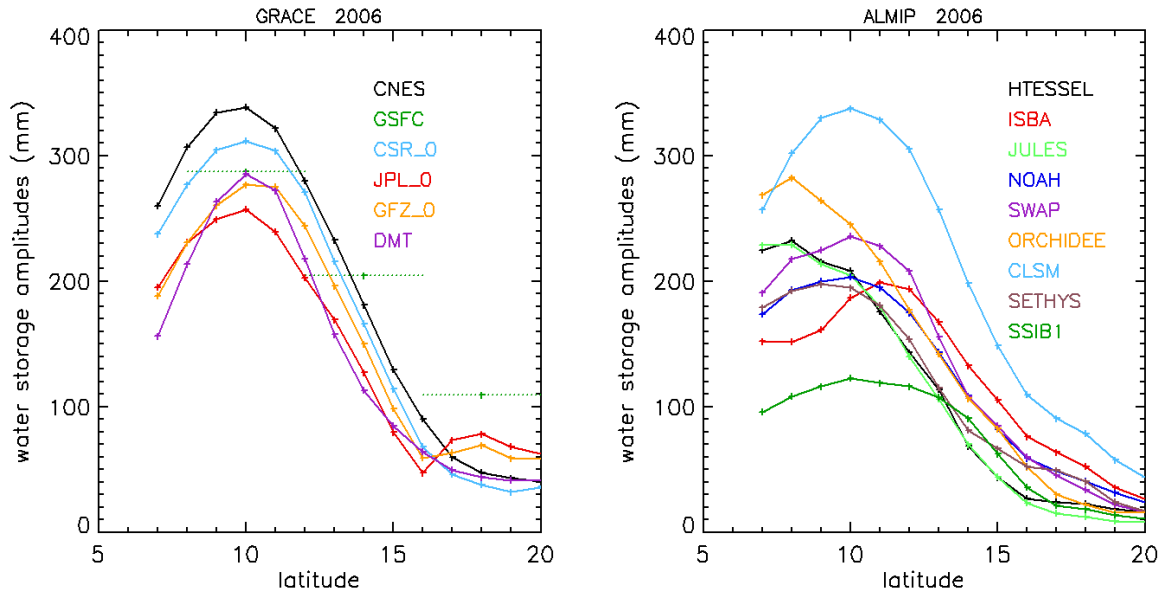


Figure 13. Latitudinal distribution (transects of 1° in latitude averaged over the full longitude extent of the study area of the annual amplitudes (difference between maximum and minimum values) in 2006 estimated by GRACE (left panel) and ALMIP models (right panel).

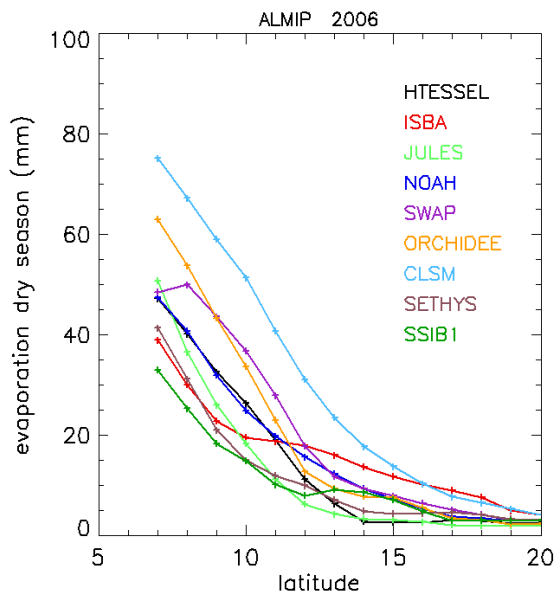


Figure 14. Latitudinal distribution of dry season (December to March) evaporation for the different ALMIP models.

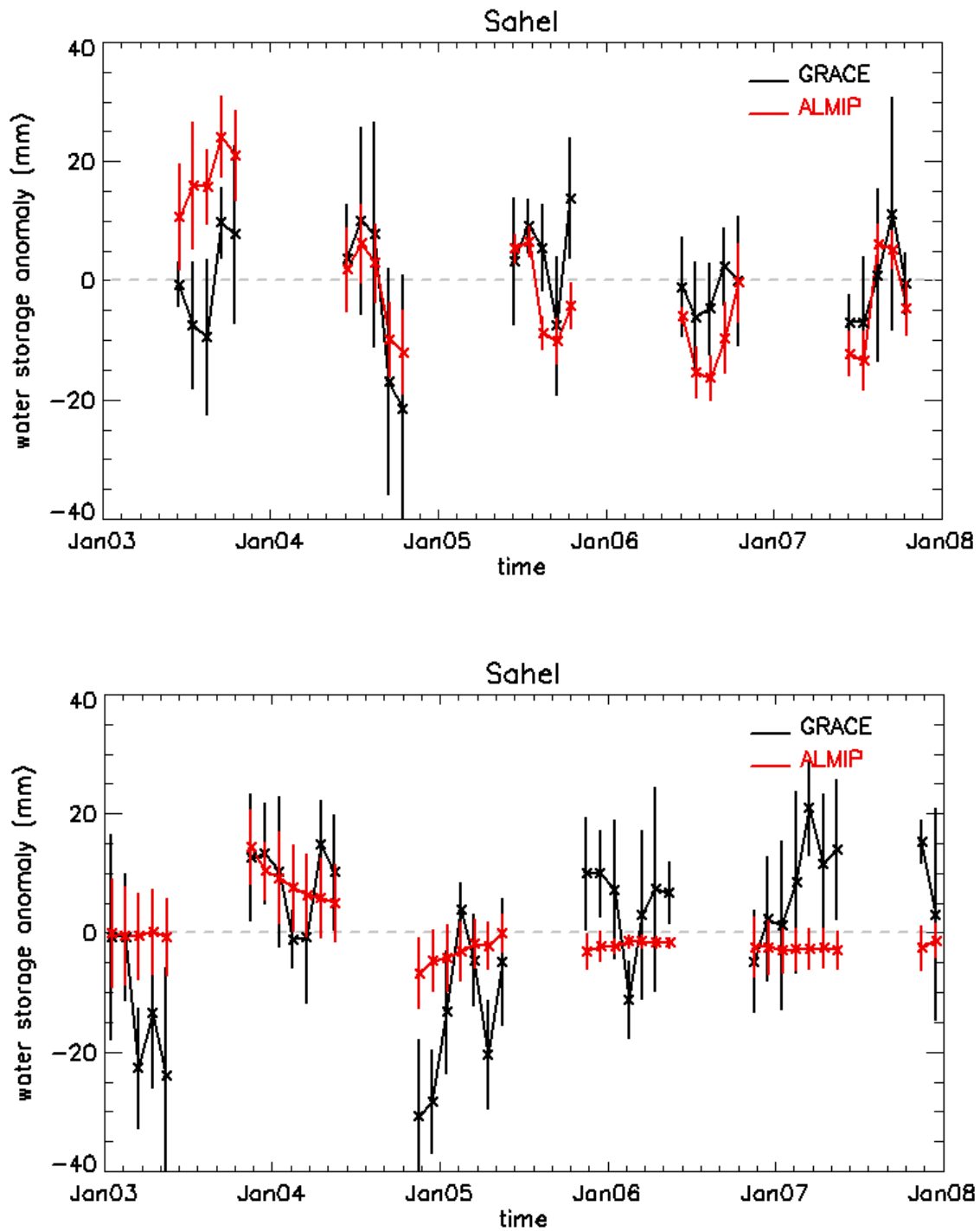


Figure 15. Interannual variations (temporal evolution minus seasonal cycle) in the water storage estimations by GRACE (multi-solutions mean and standard deviation) and ALMIP (multi-models mean and standard deviation) during the August to November (top) and December to July (bottom) periods.